NASA MEMO 12-15-58L

NASA MEMO 12-15-58L

NASA MEMORANDUM

FREE-FLIGHT INVESTIGATION OF A ROCKET-PROPELLED MODEL TO DETERMINE THE AERODYNAMIC HEATING ON A THIN, UNSWEPT, UNTAPERED, MULTISPAR, ALUMINUM-ALLOY WING AT MACH NUMBERS UP TO 2.22

By Emily W. Stephens

Langley Research Center
Langley Field, Va.

NATIONAL AERONAUTICS AND SPACE ADMINISTRATION
WASHINGTON
January 1959

NATIONAL AERONAUTICS AND SPACE ADMINISTRATION

MEMORANDUM 12-15-58L

FREE-FLIGHT INVESTIGATION OF A ROCKET-PROPELLED MODEL TO DETERMINE THE AERODYNAMIC HEATING ON A THIN, UNSWEPT, UNTAPERED, MULTISPAR, ALUMINUM-ALLOY WING AT MACH NUMBERS UP TO 2.22

By Emily W. Stephens

SUMMARY

A free-flight investigation has been made to determine some effects of aerodynamic heating on the structural behavior of a wing at supersonic speeds. The test wing was a thin, unswept, untapered, multispar, aluminum-alloy wing having a 20-inch chord, a 20-inch exposed semispan, and a circular-arc airfoil section with a thickness ratio of 5 percent. The wing was tested on a model propelled by a two-stage rocket-propulsion system to a Mach number of 2.22 and a corresponding Reynolds number per foot of 13.2×10^6.

Reasonably good agreement was obtained between Stanton numbers obtained from measured temperature-time data and values obtained by the theory of Van Driest for flat plates having turbulent boundary layers. Temperature measurements made in the skin of the wing and in the internal structures agreed well with calculated values.

The wing was instrumented to detect any apparent fluttering motion in the wing, but no evidence of flutter was observed throughout the flight.

INTRODUCTION

Results have been published (ref. 1) of a previous free-flight test in which the test wing gave no indication of flutter during flight

although flutter was evident in similar wings tested in the preflight jet of the Langley Pilotless Aircraft Research Station at Wallops Island, Va. (refs. 2 and 3). An additional model has been flown by the Langley Pilotless Aircraft Research Division to obtain the effects of aerodynamic heating on the structural behavior of a test wing at supersonic speeds. The earlier flight model had a chordwise rib located at the midspan of the wing. In an effort to induce flutter by reducing the wing stiffness, the present test wing was constructed with no chordwise rib. The test wing, a multispar aluminum-alloy wing, was mounted as one of four stabilizing wings on a two-stage rocket-propelled model and was instrumented to obtain temperature and vibration measurements. However, no evidence of wing flutter was recorded during flight and, therefore, only aerodynamic heating data are presented in this report. The wings were unswept and untapered, having a 20-inch chord, a 20-inch exposed semispan, and a circular-arc airfoil section with a thickness ratio of 5 percent. Data were recorded up to a Mach number of 2.22 and a corresponding Reynolds number per foot of 13.2×10^6.

SYMBOLS

b	length defined in figure 10(c), in.
c	specific heat of structural material (2024-T3 aluminum alloy), Btu/(lb)($^\circ$F)
c_p	specific heat of air at constant pressure, Btu/(slug)($^\circ$F)
h	local heat-transfer coefficient, Btu/(sec)(sq ft)($^\circ$F)
h'	effective heat-transfer coefficient across riveted joint, Btu/(sec)(sq ft)($^\circ$F)
h_j	joint heat-transfer coefficient, Btu/(sec)(sq ft)($^\circ$F)
k	thermal conductivity of structural material, $\text{Btu/(sec)(sq ft)}\frac{(^\circ\text{F})}{(\text{ft})}$
l	length defined in figure 10(c), in.
M	Mach number
N_{St}	Stanton number, $\frac{h}{c_p \rho V}$

N_{Pr}	Prandtl number
q	dynamic pressure, lb/sq ft
R	Reynolds number, $\frac{\rho V}{\mu} \frac{x}{12}$
t	time, sec
T	temperature, ^{o}F
V	velocity, ft/sec
x	distance from wing leading edge (measured in free-stream direction), in.
y	distance from wing tip (measured normal to model center line), in.
ρ	density, slugs/cu ft
μ	viscosity, slugs/ft-sec
τ	thickness, ft
ω	density of structural material (2024-T3 aluminum alloy), lb/cu ft

Subscripts:

AW	adiabatic wall
s	skin
stag	stagnation
w	web
∞	free-stream conditions

TEST VEHICLE AND TECHNIQUE

Model

Photographs and the general arrangement of the test vehicle are presented in figures 1 to 3, and the geometry and dimensions of the

test wing are presented in figure 4. The instrumented wing was one of four stabilizing wings mounted symmetrically on the test vehicle. The wings were the same in all respects except stiffness. The test wing had the same design as wings tested in the preflight jet (refs. 2 and 3) which had no chordwise ribs; however, the remaining three model wings were stiffened by means of three chordwise ribs per wing to minimize the possibility of failure of the noninstrumented wings. The wings were unswept and untapered, having a 20-inch chord, a 20-inch exposed semispan, and a circular-arc airfoil section with a thickness ratio of 5 percent. The wings were constructed of 2024-T3 aluminum alloy and had 0.064-inch-thick skins, six 0.025-inch-thick internal spars, a solid 0.25-inch-thick wing-tip bulkhead, and solid leading- and trailing-edge sections. All rivet heads were ground flush with the wing surface and the entire surface of the test wing was finished to a roughness of approximately 35 microinches.

Reference 1 gives a detailed description of a wing previously flight tested as part of this investigation. The wing of reference 1 differed from the wing described in this report in that it had greater stiffness which was contributed by one chordwise rib located at the center of the wing.

In addition, three wings (MW-2, MW-2-(2), and MW-2-(3)) identical to the present wing were tested at $M \approx 2.0$ (refs. 2 and 3) in the preflight jet at Wallops Island, Va.

Test-Vehicle Instrumentation

A detailed sketch of wing instrumentation is presented in figure 5.

Wing temperatures were measured with six No. 30 iron-constantan thermocouples located 4.8 inches inboard of the wing tip. Three thermocouples were located in the skin midway between the spanwise spars, one thermocouple was located on the center line of a web located 13.6 inches from the wing leading edge, one thermocouple was located on the wing-chord plane of the solid-wedge portion of the wing leading-edge section, and one thermocouple was located in a corresponding position in the solid-wedge portion of the wing trailing-edge section. The method used to install the thermocouples and record temperature measurements is given in detail in reference 1.

Since several wings identical to the flight-tested wing had either fluttered or, in one case, fluttered and failed during tests in the preflight jet (refs. 2 and 3), the present wing was instrumented with three strain gages and a vibrometer (miniaturized accelerometer). These flutter detectors, located as shown in figure 5, were considered adequate to detect any fluttering motion apparent in the wing during flight.

The strain gages used were uncalibrated Baldwin-Lima-Hamilton EBD-1D gages wherein the telemeter oscillator was adjusted for maximum sensitivity in order to detect relatively small wing deflections. The telemeter range was such that the ground-station galvanometer would register full deflection when design bending moment was applied. The vibrometer, though not so sensitive to small disturbances as the strain gages, was included as an independent means of flutter detection and was more suited for the measurement of violent wing motions should they occur.

In addition, telemeter data were obtained of longitudinal acceleration and dynamic pressure.

Flight-Test Technique

The model was propelled by a two-stage rocket-propulsion system. The first stage was comprised of two 2.8-KS-9300 Cajun rocket motors strapped together and fired simultaneously. A JATO, 6-KS-3000, T40 rocket motor was employed as the sustainer rocket. The model was intended to maintain a constant Mach number of approximately 2.0 for several seconds of its trajectory. This Mach number was not maintained, however, since the loss of a booster fin near burnout of the first-stage rocket disturbed the model from its intended flight path and caused the model to follow a higher altitude trajectory than intended. A Mach number of approximately 2.07 was reached at burnout of the first-stage rocket (3.15 seconds), after which the model coasted for 1.60 seconds before being accelerated to a peak Mach number of approximately 2.22 at burnout of the second-stage sustainer rocket (10.55 seconds). The model followed an essentially zero-lift trajectory throughout the flight.

A time history of velocity was obtained by a CW Doppler radar. Other instrumentation included an NACA modified SCR-584 radar used to obtain space coordinates of the model in flight and a radiosonde launched immediately after the test flight and tracked by a Rawin set AN/GMD-1A used to determine atmospheric data and wind conditions.

Time histories of several important flight test parameters are presented in figure 6. An altitude of approximately 7,000 feet was obtained at peak Mach number.

Precision

The maximum errors which exist in these test data were estimated to be as follows:

T_s, °F	±5
T_∞, °F	±5
V_∞, ft/sec	±4.0
ρ, slug/cu ft	±0.0003
M	±0.01

RESULTS AND DISCUSSION

Temperature measurements were made with thermocouples at several locations in the internal structure of the wing as well as in the skin. These thermocouple data are presented as temperature-time histories. Comparisons are shown between measured temperatures and calculated temperatures. With the exception of minor wing disturbances which occurred at booster-fin breakup, no evidence of wing flutter was recorded during the flight test by either the strain gages or vibrometer.

Skin and Internal Temperatures

Temperature-time histories obtained from thermocouple data are presented in figure 7. Thermocouple measurements were made at three locations in the outer skin of the test wing, at the center line of a spanwise web located at the wing 0.68 chord and on the wing-chord plane of the solid-wedge sections of the wing leading and trailing edges. Figure 8 shows the chordwise variations of the measured skin temperatures and of theoretical temperatures calculated by use of numerical integration at several typical times. For purposes of this figure the temperature variation near the spars has been ignored since reference 1 has shown the effect of conduction on surface temperatures to be small for the conditions of this test. The theoretical values, obtained by the turbulent flat-plate theory of Van Driest (ref. 4), show reasonably good agreement with the measured values.

Calculations were made to estimate analytically the temperatures in the solid leading- and trailing-edge sections of the wing and in a spanwise web, and these calculated values were then compared with measured temperatures at the same wing locations (fig. 9). The method used to calculate the temperatures is described in detail in the appendix. For purposes of calculation the cross sections of the wing were divided into segments as shown in figure 10 and heat-balance equations were set up for each block. Temperatures calculated by the digital computer for the internal structures of the test wing showed good agreement with measured values.

Heat Transfer

The measured temperature-time data were reduced to Stanton numbers and are compared in figure 11 with values obtained by the theory of Van Driest for a flat plate with laminar and turbulent boundary layers. The laminar values were computed by the method of reference 5. The turbulent values were computed by the method of reference 4 in which the Von Kármán similarity law for mixing length and a Reynolds analogy factor based upon laminar and turbulent Prandtl numbers equal to 0.71 and 0.86, respectively, are assumed. Theoretical values of recovery factor equal to $(N_{Pr})^{1/3}$ and a constant ratio of Stanton number to skin-friction coefficient equal to 0.60 were used in the calculations of the turbulent values of Stanton number.

Local aerodynamic conditions, obtained from measured free-stream data by two-dimensional shock-expansion theory, were used for both the experimental and theoretical calculations. No attempt was made to correct for three-dimensional effects as previous experience has shown these effects to be negligible for test conditions similar to these.

The equation used to reduce the measured temperature data to Stanton number is:

$$N_{St} = \frac{\frac{\Delta T_s}{\Delta t} c\omega\tau \Big/ (T_{AW} - T_s)}{\rho V c_p}$$

Little credence can be attached to values of Stanton numbers obtained from measured temperature-time curves between 11 and 13 seconds. In this region the values of the forcing function $T_{AW} - T_s$ and slope $\Delta T_s/\Delta t$ are small and account for large inaccuracies in the Stanton numbers. The overall trend of the measured values, though somewhat lower, agrees reasonably well with the theoretical turbulent-boundary-layer values.

Within the accuracy of measuring heat transfer, the agreement of the data of the current model and the data of a similar model (ref. 1) with turbulent theory is about the same, with slightly closer approximation obtained for the model of reference 1.

Comparison With Preflight-Jet Tests

Temperature data and Stanton numbers for the flight model are compared with data obtained by the Langley Structures Research Division in ground tests of identical wings tested in the preflight jet of the

Langley Pilotless Aircraft Research Division. Jet conditions were held approximately constant during testing at a stagnation temperature of 500° F and a dynamic pressure of approximately 6,000 pounds per square foot.

Three wings, identical to the present test wing, were tested in the preflight jet. One of the ground-tested wings fluttered and failed during testing; a second wing fluttered near the end of the test during each of three runs; the third wing gave no indication of flutter. Figure 13 presents a comparison of temperatures recorded in flight with temperatures recorded in the preflight jet at approximately the same location on the test wing. An envelope is employed to include the range of temperatures encountered in the preflight jet. Little temperature rise occurred during the first 2 seconds of the flight test when the model was flying at subsonic Mach numbers, whereas instantaneous heat rise occurred during testing in the preflight jet. Consequently, the temperature-time curve from the preflight jet was shifted 2 seconds to illustrate better the relation between the two curves during the heating cycle. The maximum temperatures measured in the preflight jet averaged 100° higher than the maximum temperature attained by the flight model. The temperature range at which the wings fluttered in the preflight jet has been indicated in figure 12. These temperatures were not attained in flight. The heating rate for the flight model during the first half of sustainer firing time was less than that for the ground tests at comparable times. Later, the heating rates for flight and ground tests were comparable.

As a matter of interest the flight and ground test data are compared in figure 13 using the turbulent-flow correlating factor $N_{St}\sqrt[5]{R}$. For constant Mach number, turbulent theory gives $N_{St}\sqrt[5]{R}$ as essentially constant when plotted as a function of Reynolds number. The data of this figure show that the heat-transfer coefficients obtained for both the flight and preflight-jet tests are essentially constant and of the same magnitude. These experimental values are lower than theoretical values based on the nomograph of reference 4.

CONCLUSIONS

Temperature-time measurements were made on a multispar, untapered, unswept, aluminum-alloy wing in free flight up to a Mach number of 2.22 and a corresponding Reynolds number per foot of 13.2×10^6. These data were compared with theory and with other data obtained in flight and in ground tests. The following conclusions were indicated:

1. Stanton numbers obtained from measured temperature-time data agree fairly well with theoretical values calculated by the theory of Van Driest for flat plates having turbulent boundary layers.

2. Temperatures calculated for both the wing skin and internal structures closely approximate measured values.

3. No evidence of flutter was indicated in the present test. However, no direct comparison can be made between wings tested in the preflight jet where flutter did occur and wings tested in flight since a higher heating rate, higher temperatures, and a higher dynamic pressure were obtained in the preflight jet.

12-15-58L

Langley Research Center,
National Aeronautics and Space Administration,
Langley Field, Va., October 1, 1958.

APPENDIX

CALCULATIONS OF TEMPERATURES FOR INTERNAL WING STRUCTURES

In an effort to estimate temperatures which would result from flight conditions imposed in the current test, calculations have been made by the IBM type 704 electronic data processing machine of the Langley Analytical Computing Branch of the internal temperatures occurring at the wing-chord plane in the solid wing leading- and trailing-edge sections and at the center line of a spanwise web. For purposes of calculation the cross sections of the wing were divided as shown in figure 10 and heat-balance equations were set up for each block. Finite differences in temperature for each block were solved for by making simultaneous solutions of these heat-balance equations over the desired time range. At any given time of the calculations the material properties were assumed to remain constant.

The heat-balance equations included terms for heat transfer by conduction and convection. The effects of radiation were not included in these calculations as they were considered to be negligible over the temperature range encountered in the flight test.

Values of heat-transfer coefficients and adiabatic wall temperatures used to calculate temperatures in the wing leading- and trailing-edge sections were based on local flow conditions and the theory of Van Driest for turbulent boundary layers. In order to calculate the temperatures at the web center line, heat-transfer coefficients and adiabatic wall temperatures based on measured temperature-time data were used to determine heat transmitted to the outer skin. Heat-transfer coefficients were calculated for the end blocks of the outer surface of the wing cross sections, and the values for intermediate blocks were obtained by linear interpolation. An interface conductance value (h_j = 300) corresponding to a riveted aluminum-aluminum structure at the average wing temperature encountered during flight (T = 180° F) was chosen from figure 11 of reference 6.

The following examples of heat-balance equations for several blocks of the wing web section (fig. 10(c)) are typical for unit spanwise distance:

(1) Block 3:

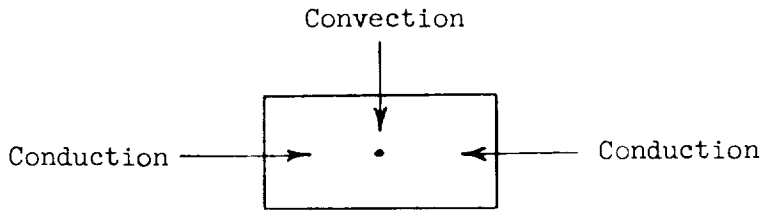

$$\Delta T_3 = \frac{\Delta t}{\tau_3 b_3 \omega c_3}\left[h_3 b_3 (T_{AW} - T_3) + \frac{k_3 \tau_s (T_2 - T_3)}{l_{2-3}} + \frac{k_3 \tau_s (T_4 - T_3)}{l_{3-4}}\right]$$

(The symbols b and l are defined in figure 10(c). Numbers used as subscripts refer to block numbers.)

(2) Block 6:

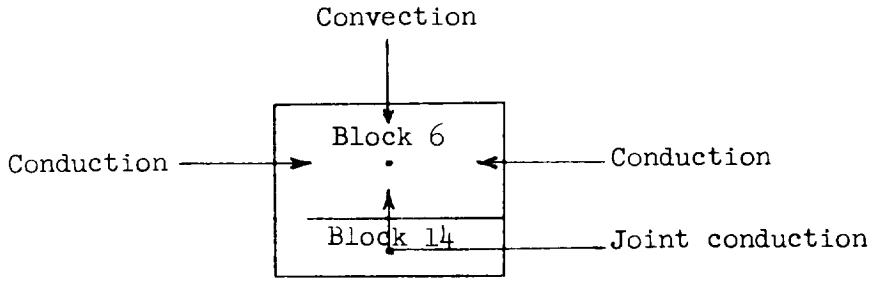

$$\Delta T_6 = \frac{\Delta t}{\tau_6 b_6 \omega c_6}\left[h_6 b_6 (T_{AW} - T_6) + \frac{k_6 \tau_s (T_5 - T_6)}{l_{5-6}} + \frac{k_6 \tau_s (T_7 - T_6)}{l_{6-7}} + h' b_6 (T_{14} - T_6)\right]$$

where $h' = \dfrac{2}{\frac{2}{h_j} + \frac{\tau_{14}}{k_{14}} + \frac{\tau_6}{k_6}}$ (see ref. 7).

(3) Block 16:

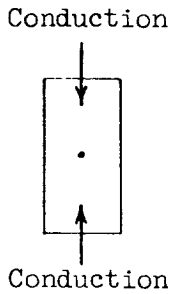

$$\Delta T_{16} = \frac{\Delta t}{\tau_{16} b_{16} \omega c_{16}} \left[\frac{k_{16} \tau_w (T_{15} - T_{16})}{l_{15\text{-}16}} + \frac{k_{16} \tau_w (T_{17} - T_{16})}{l_{16\text{-}17}} \right]$$

The time increment, equal to 0.5 second, and block sizes used in these calculations were considered to be of appropriate size to yield sufficient accuracy. These values may differ, however, with different heating rates and material properties.

REFERENCES

1. Strass, H. Kurt, and Stephens, Emily W.: Aerodynamic Heating of a Thin, Unswept, Untapered, Multiweb, Aluminum-Alloy Wing at Mach Numbers Up to 2.67 As Determined From a Free-Flight Investigation of a Rocket-Propelled Model. NACA RM L57F06, 1957.

2. Griffith, George E., Miltonberger, Georgene H., and Rosecrans, Richard: Tests of Aerodynamically Heated Multiweb Wing Structures in a Free Jet at Mach Number 2 - Two Aluminum-Alloy Models of 20-Inch Chord With 0.064- and 0.081-Inch-Thick Skin. NACA RM L55F13, 1955.

3. Miltonberger, Georgene H., Griffith, George E., and Davidson, John R.: Tests of Aerodynamically Heated Multiweb Wing Structures in a Free Jet at Mach Number 2 - Two Aluminum-Alloy Models of 20-Inch Chord With 0.064-Inch-Thick Skin at Angles of Attack of 0° and $\pm 2^{\circ}$. NACA RM L57H19, 1957.

4. Van Driest, E. R.: The Problem of Aerodynamic Heating. Aero. Eng. Rev., vol. 15, no. 10, Oct. 1956, pp. 26-41.

5. Van Driest, E. R.: Investigation of Laminar Boundary Layer in Compressible Fluids Using the Crocco Method. NACA TN 2597, 1952.

6. Barzelay, Martin E., Tong, Kin Nee, and Holloway, George F.: Thermal Conductance of Contacts in Aircraft Joints. NACA TN 3167, 1954.

7. Griffith, George E., and Miltonberger, Georgene H.: Some Effects of Joint Conductivity on the Temperatures and Thermal Stresses in Aerodynamically Heated Skin-Stiffener Combinations. NACA TN 3699, 1956.

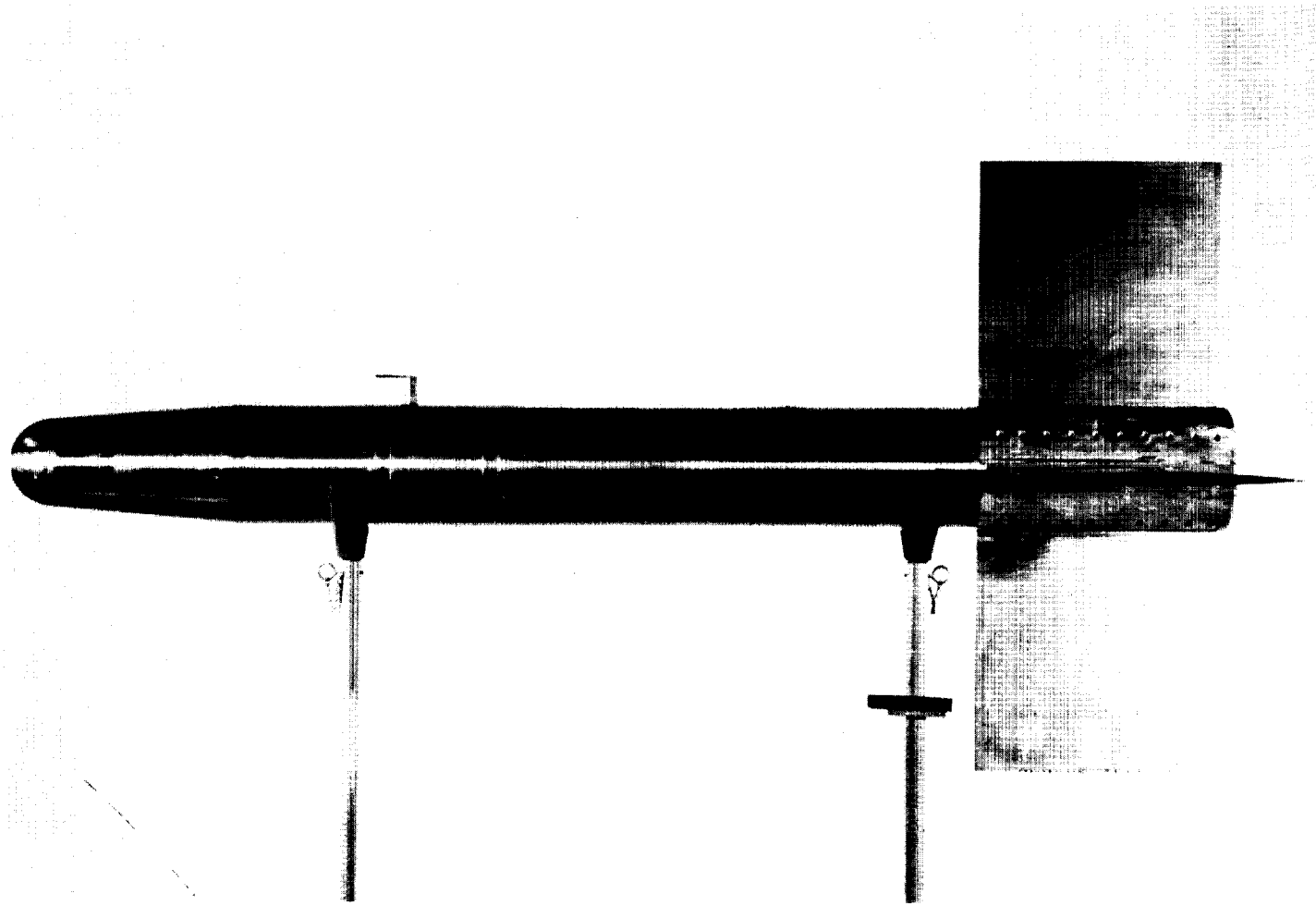

(a) Side view. L-57-4759.1

Figure 1.- Photograph of test vehicle.

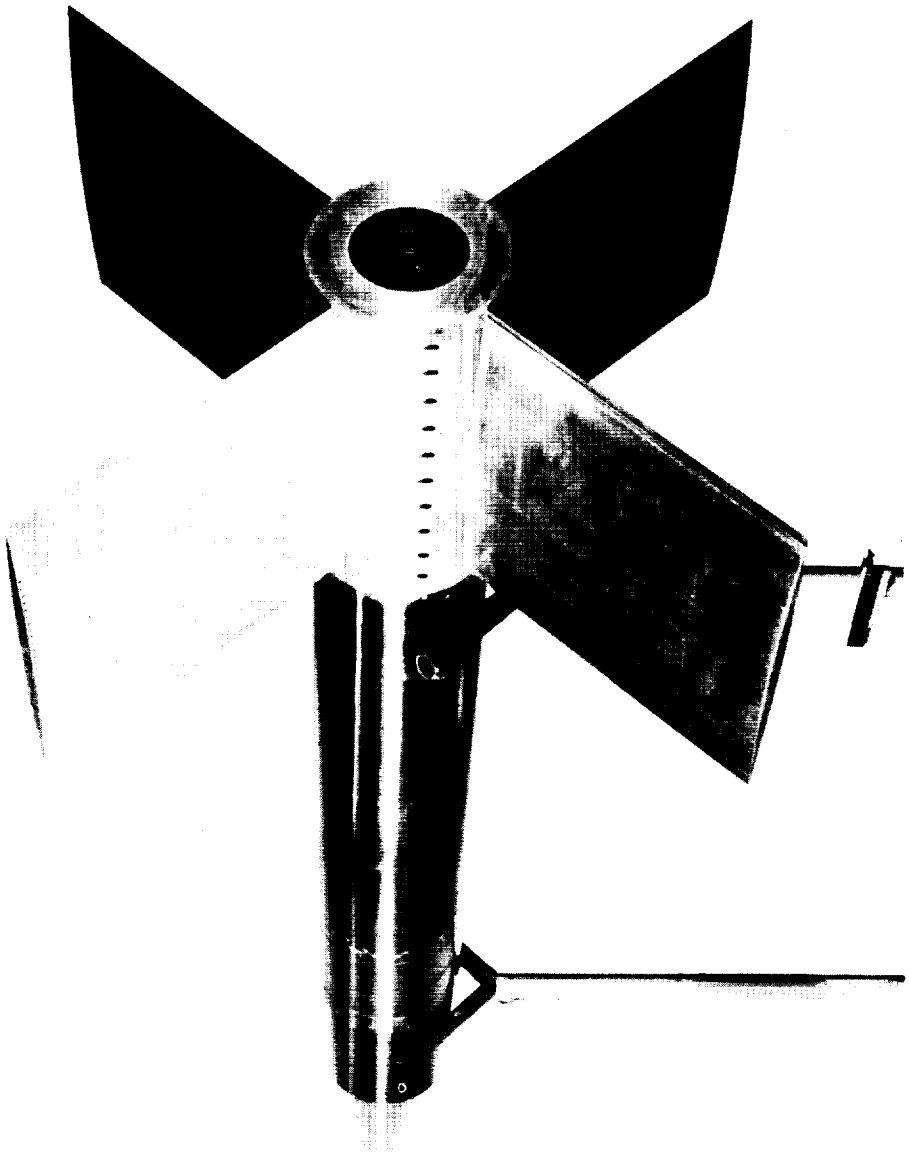

(b) Rear view. L-57-4761.1

Figure 1.- Concluded.

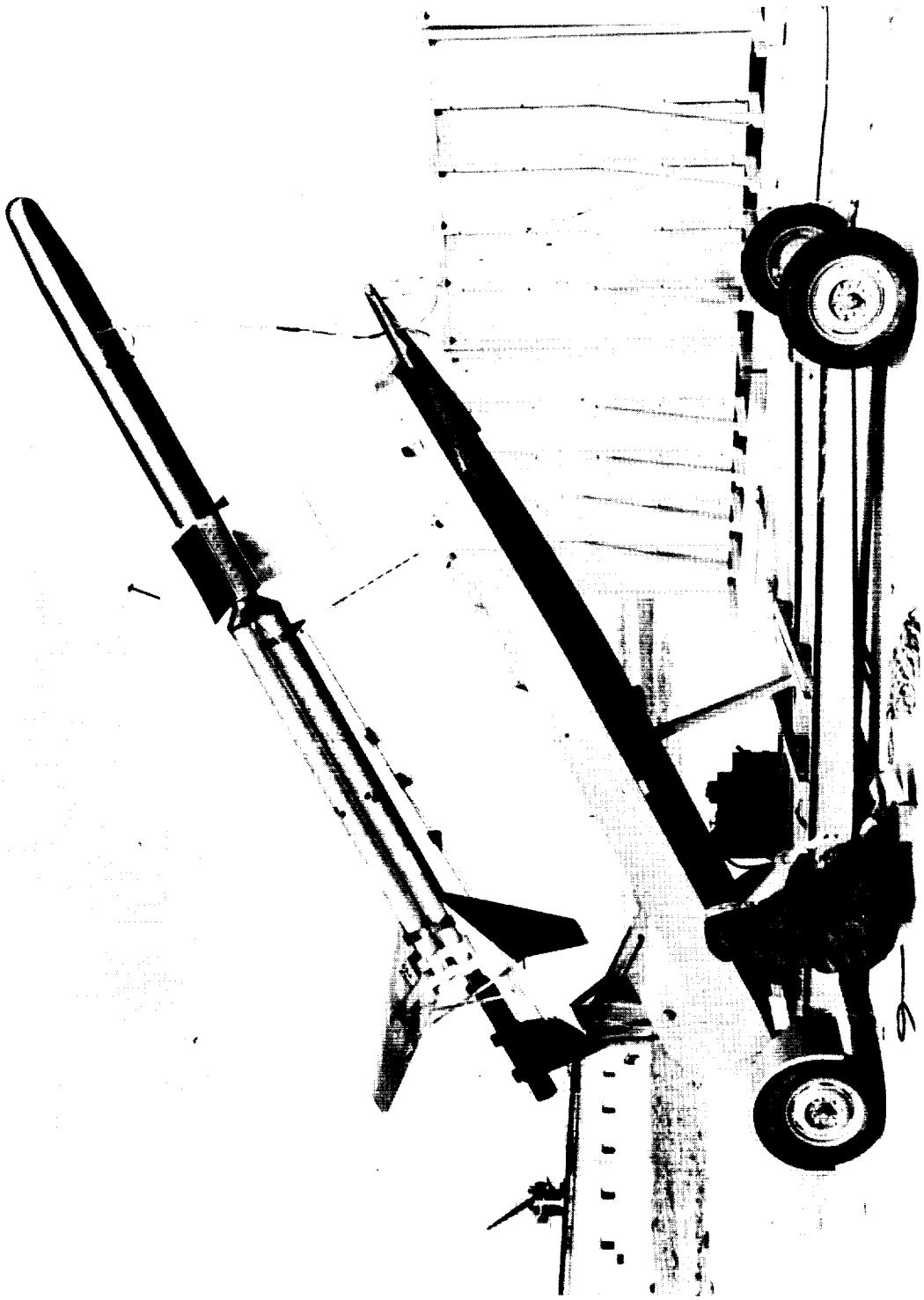

Figure 2.- Rocket model on launcher. L-57-5187.1

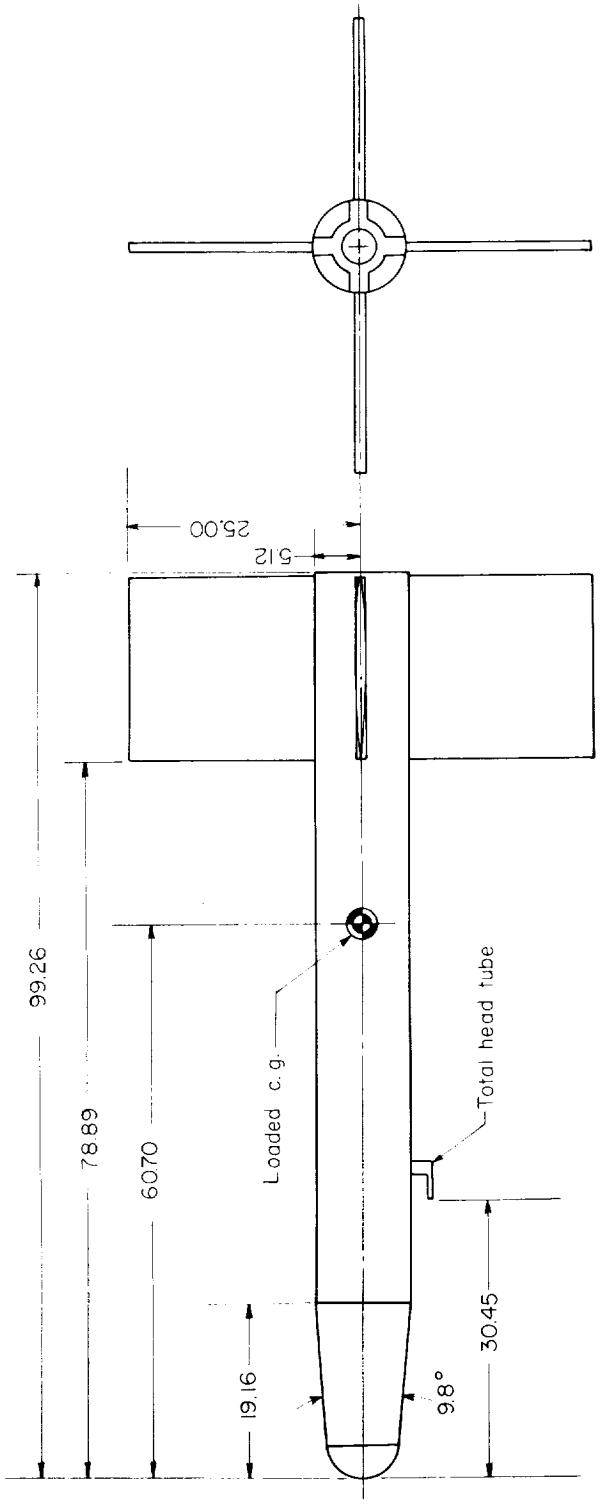

Figure 3.- General arrangement of structural test vehicle. All dimensions are in inches.

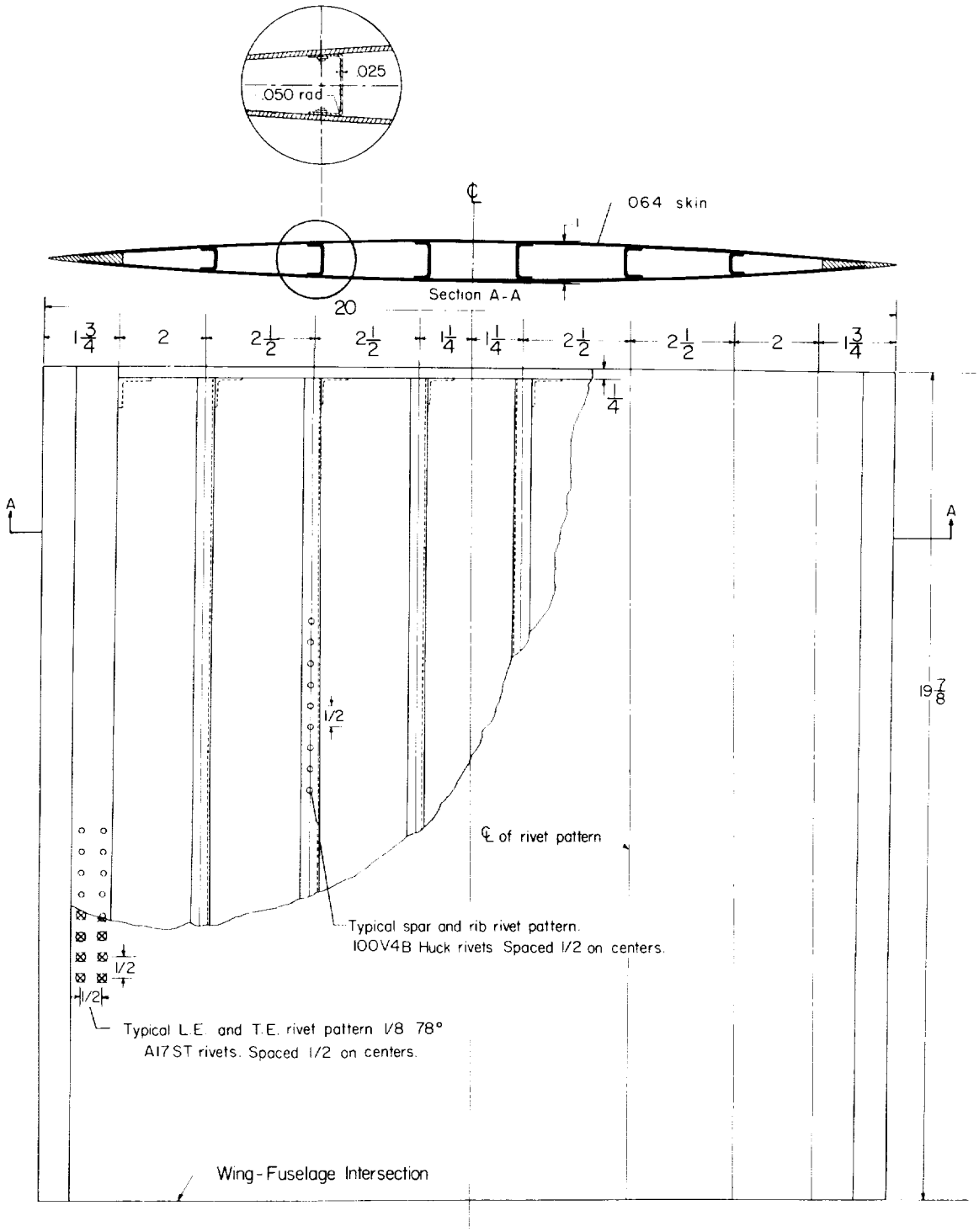

Figure 4.- Dimensions of test wing. All dimensions are in inches.

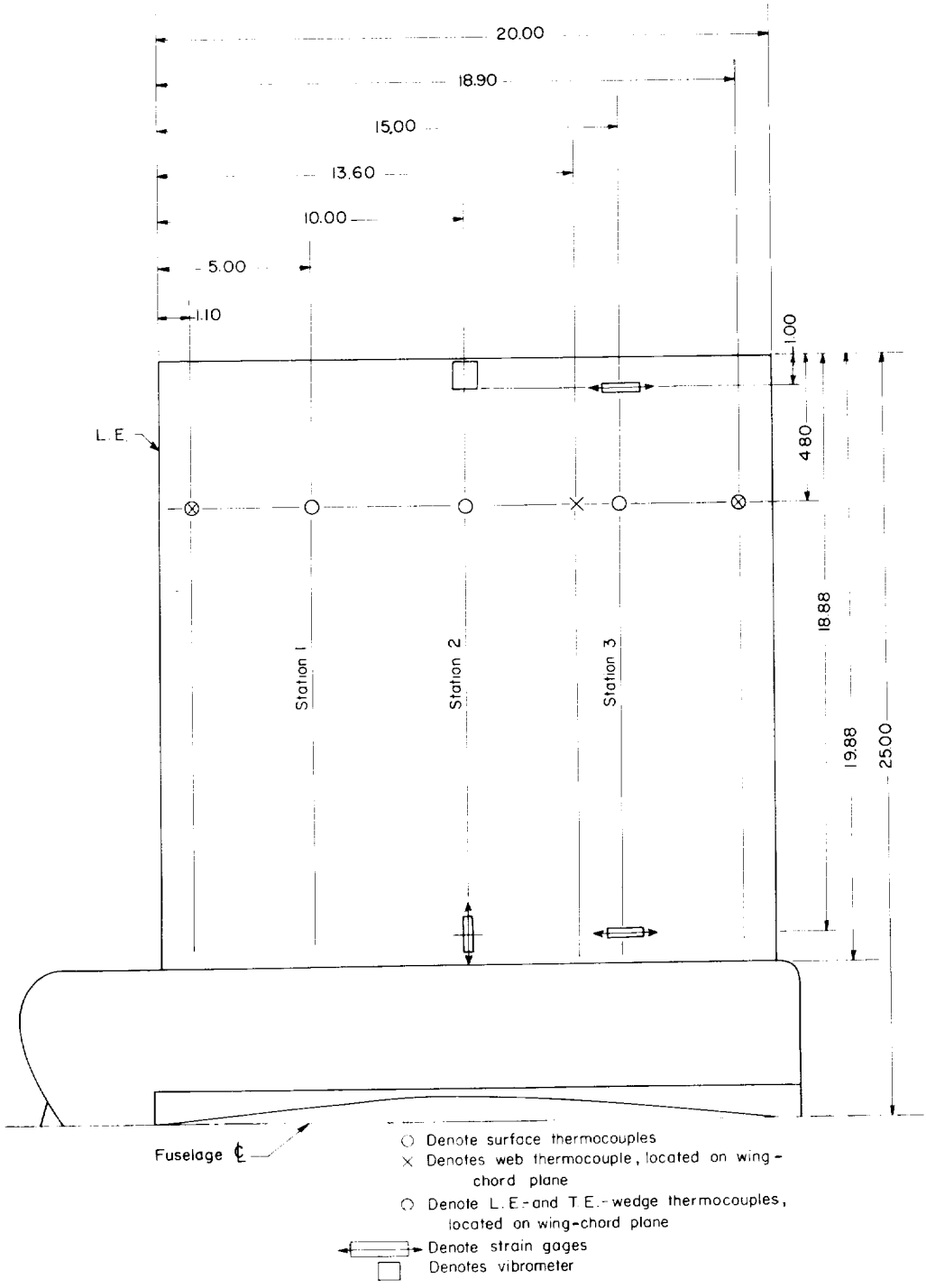

Figure 5.- Instrumentation of test wing of flight model. All dimensions are in inches.

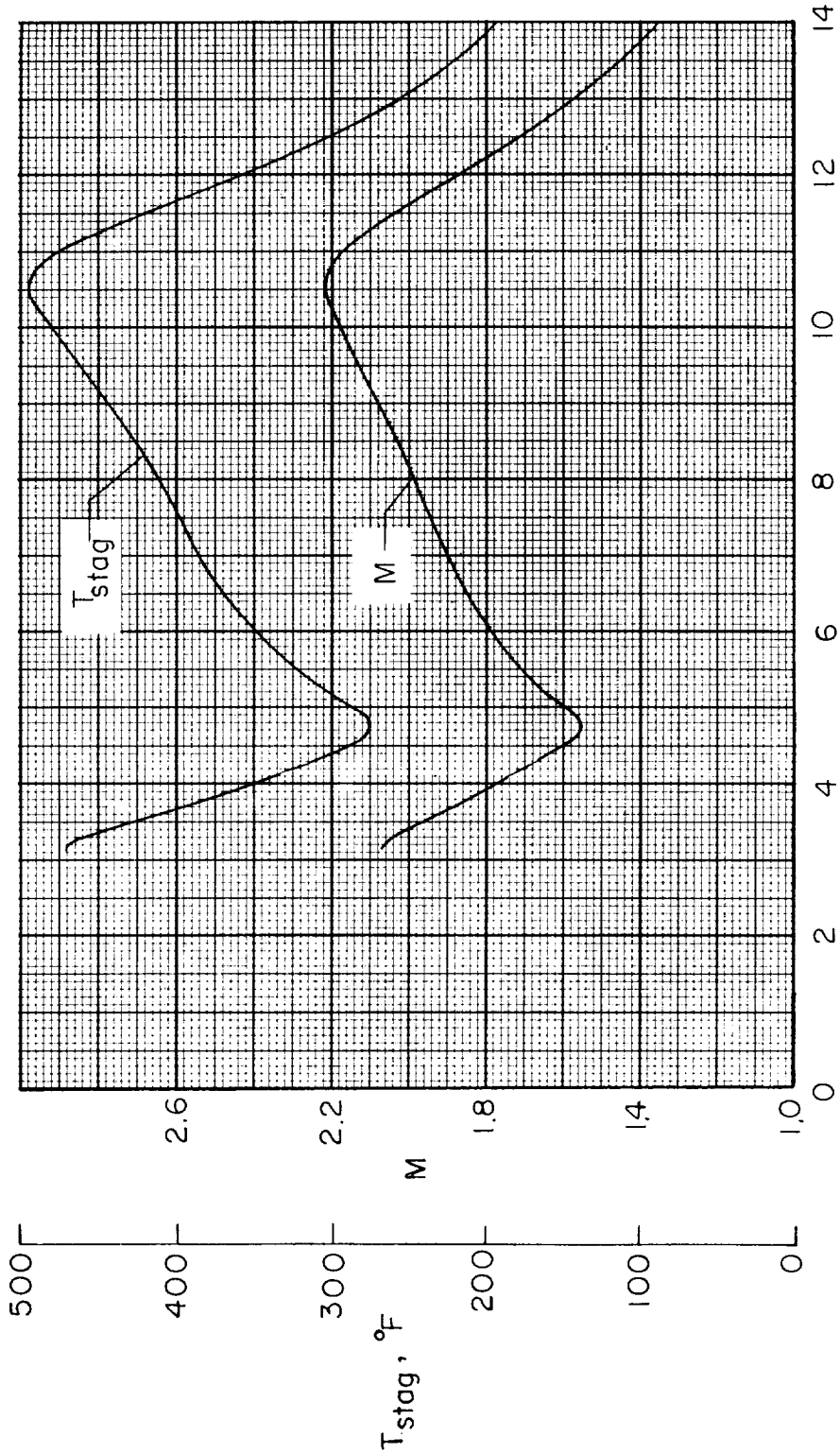

(a) Variation of stagnation temperature and Mach number with time.

Figure 6.- Time histories of several important flight parameters.

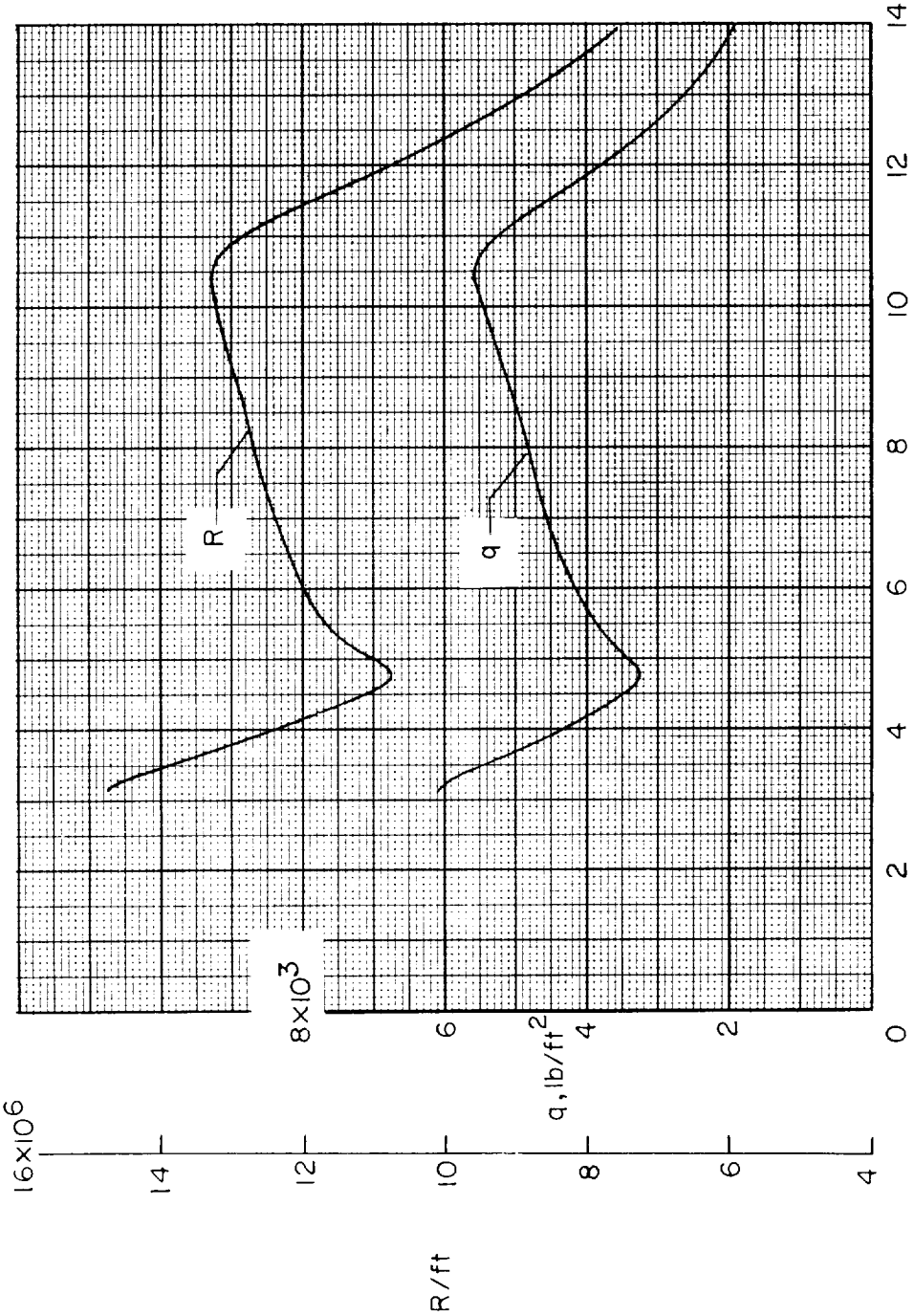

(b) Variation of Reynolds number and dynamic pressure with time.

Figure 6.- Concluded.

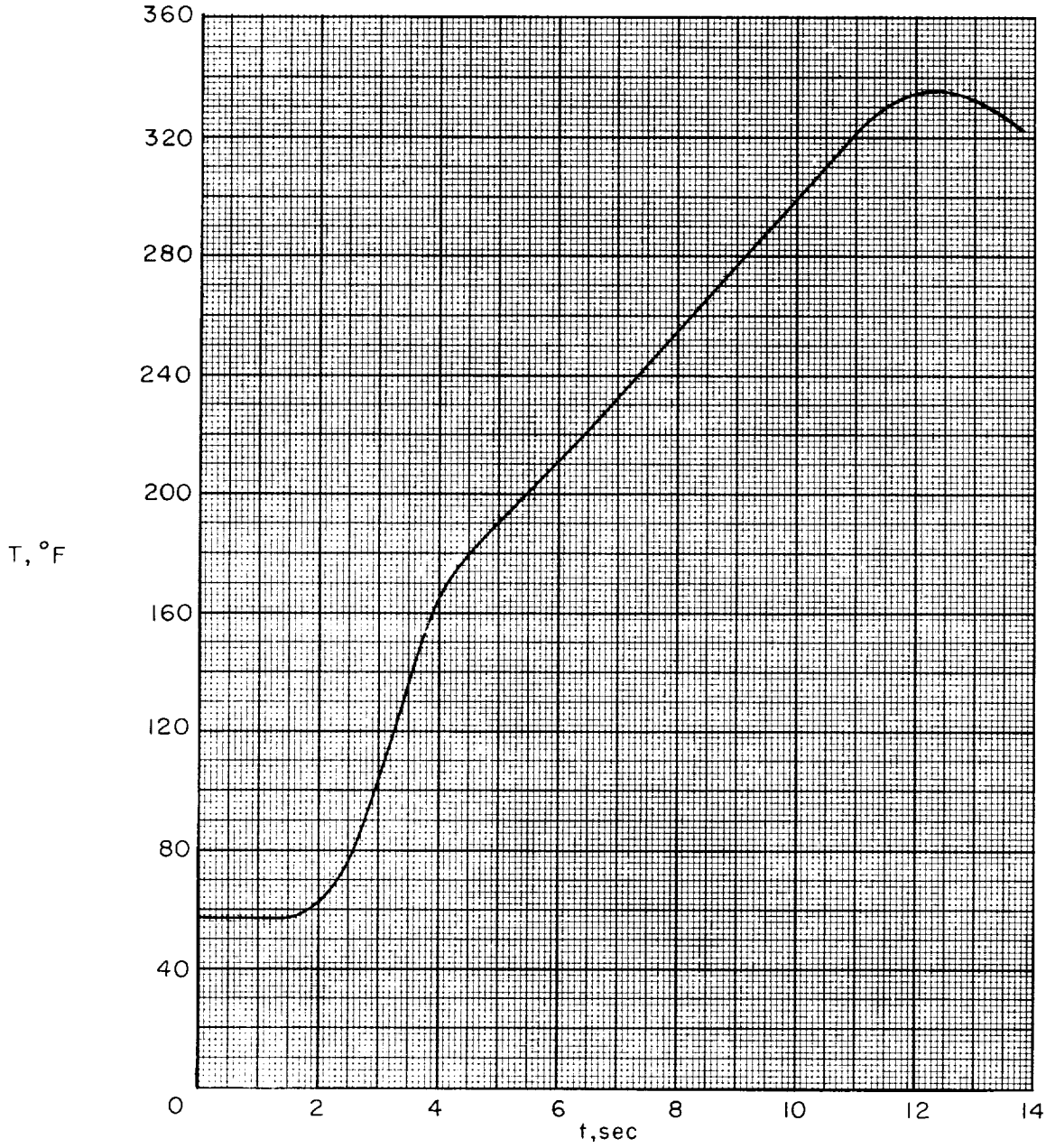

(a) Leading-edge wedge.

Figure 7.- Variation of measured temperatures with time for various chordwise stations.

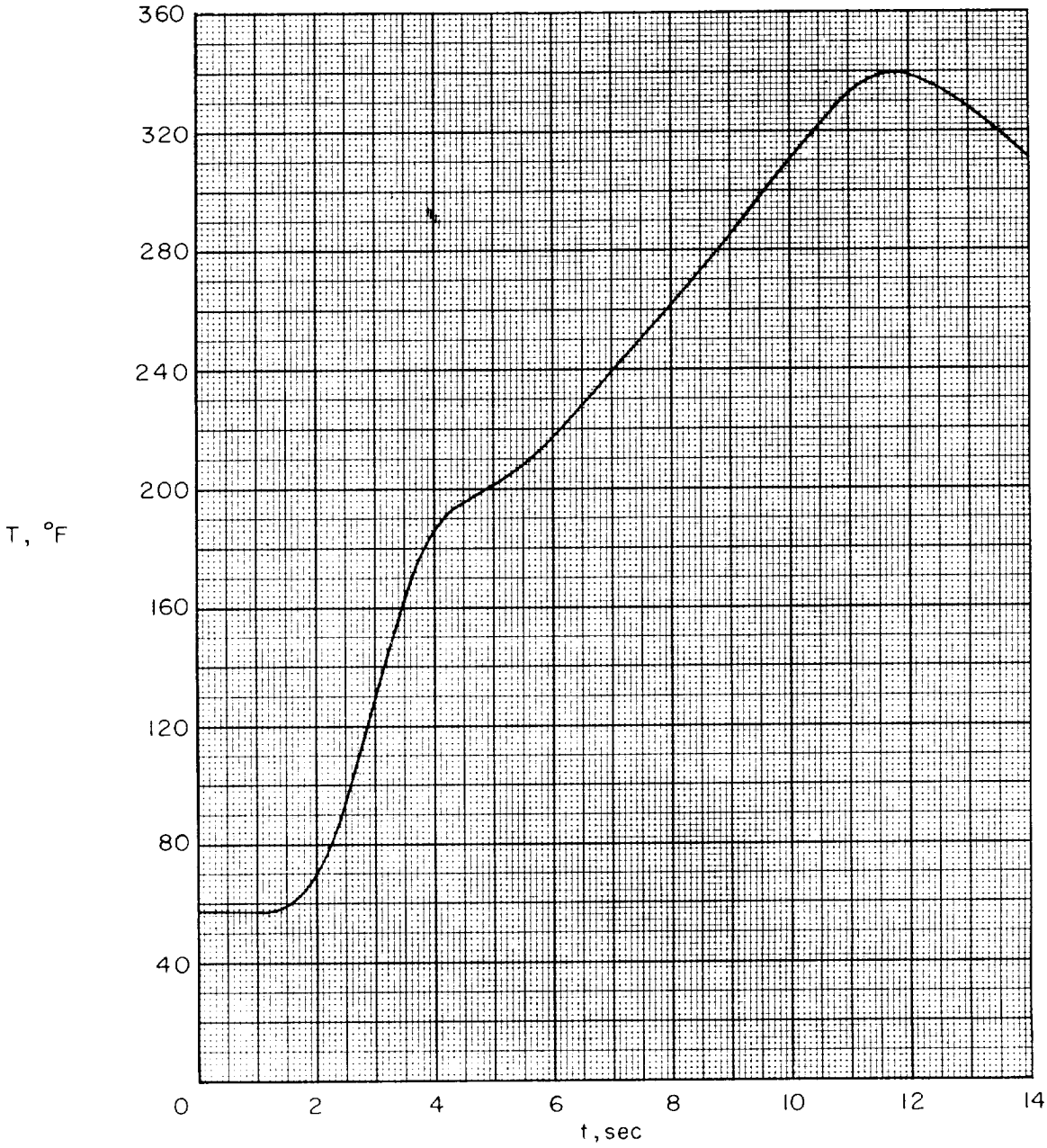

(b) Station 1.

Figure 7.- Continued.

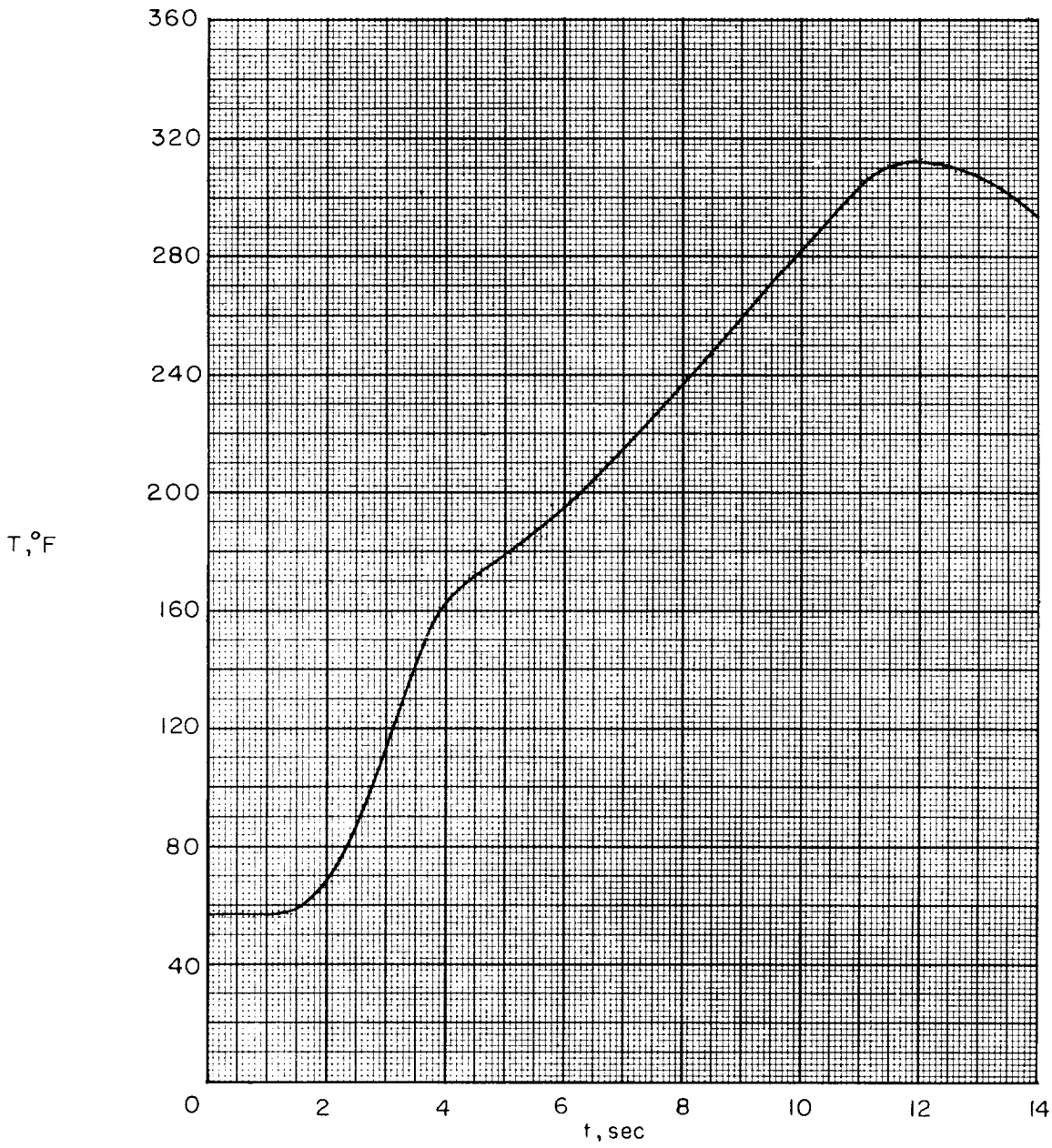

(c) Station 2.

Figure 7.- Continued.

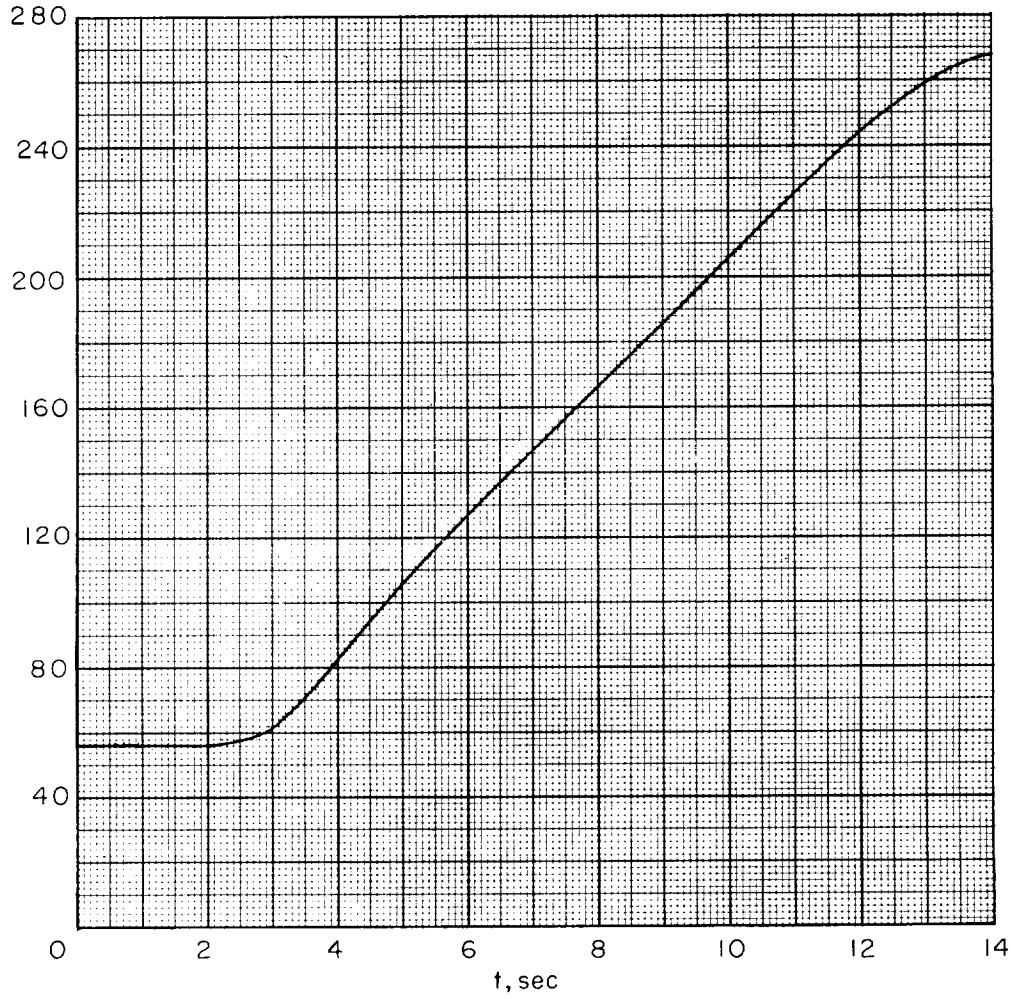

(d) Web.

Figure 7.- Continued.

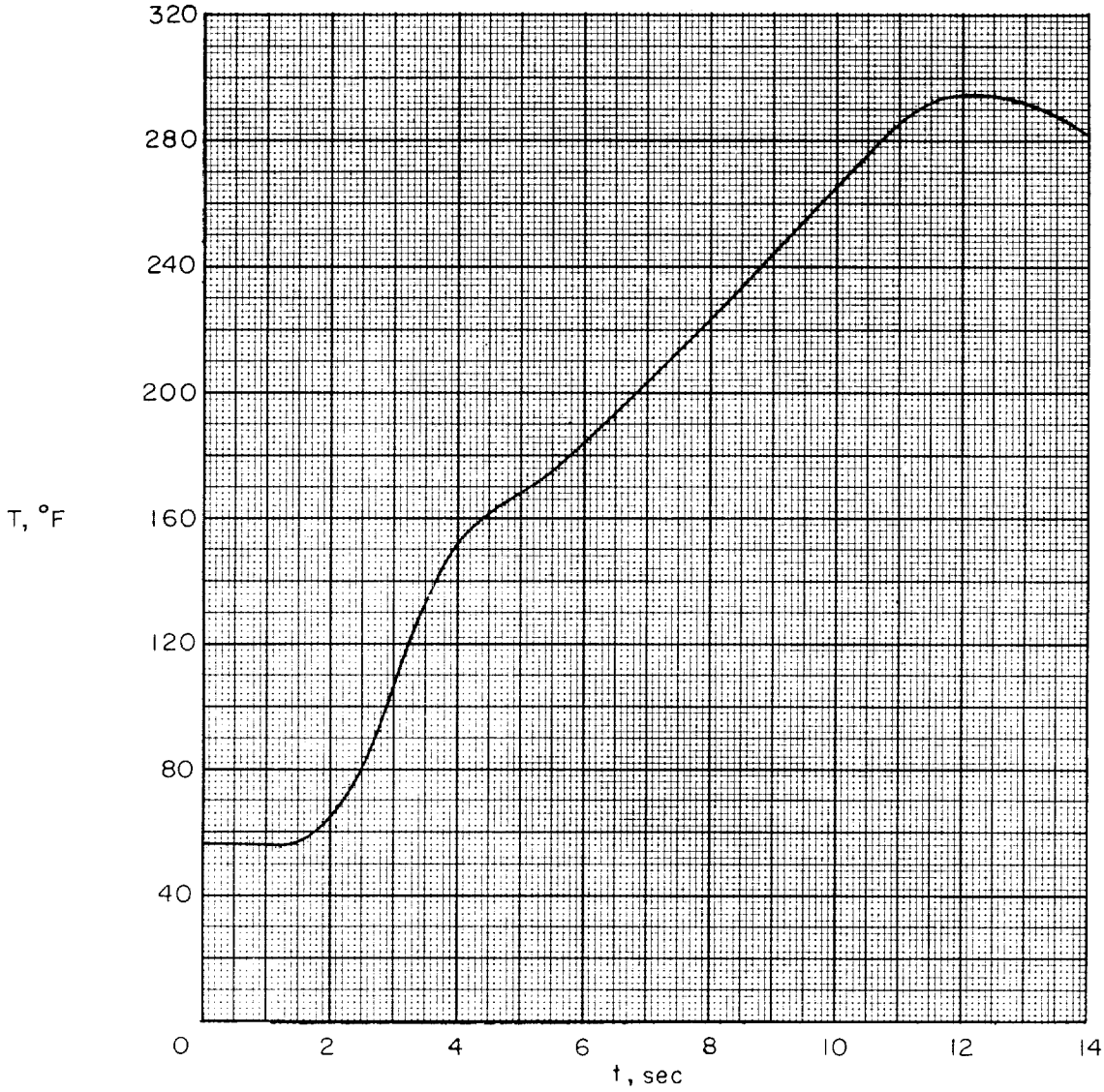

(e) Station 3.

Figure 7.- Continued.

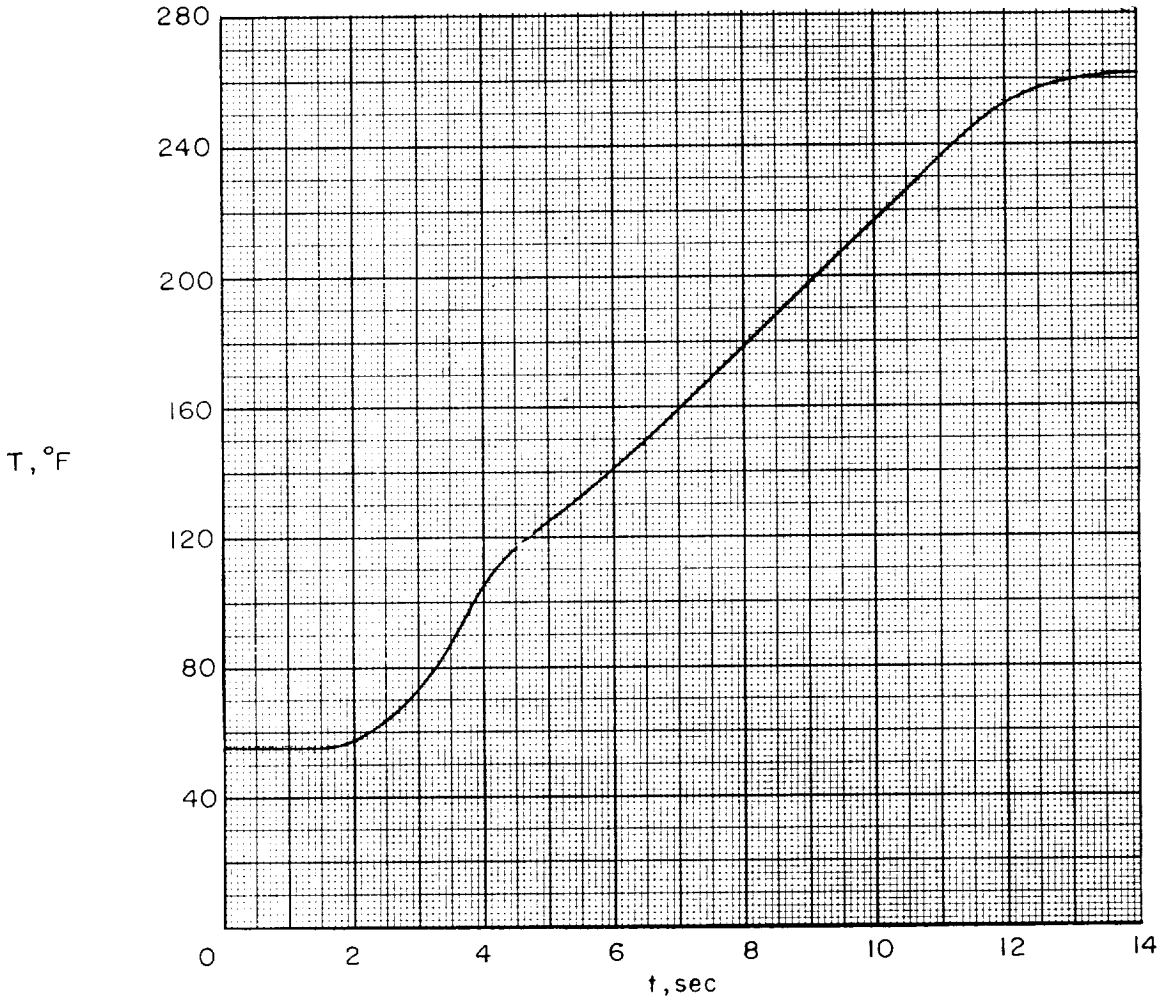

(f) Trailing-edge wedge.

Figure 7.- Concluded.

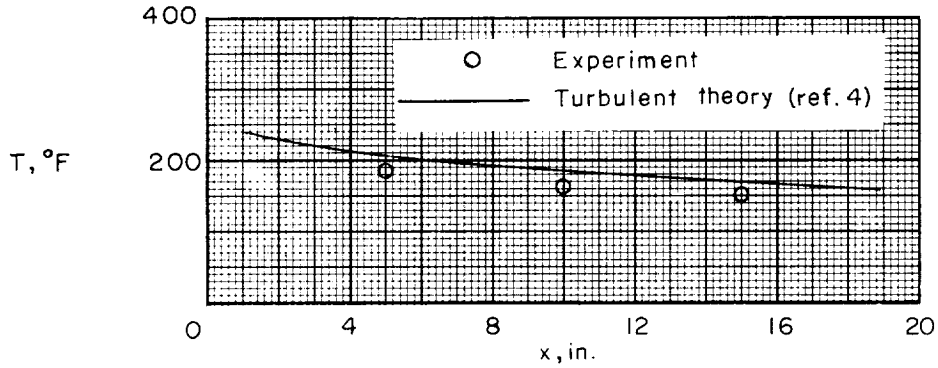

(a) t = 4 seconds; M = 1.77.

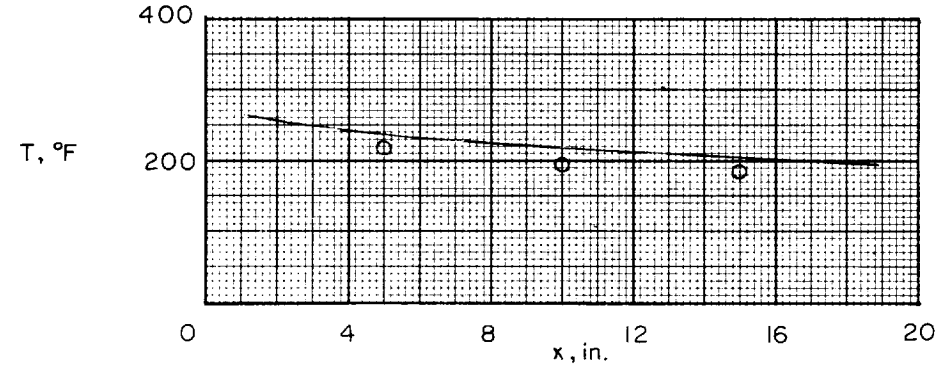

(b) t = 6 seconds; M = 1.79.

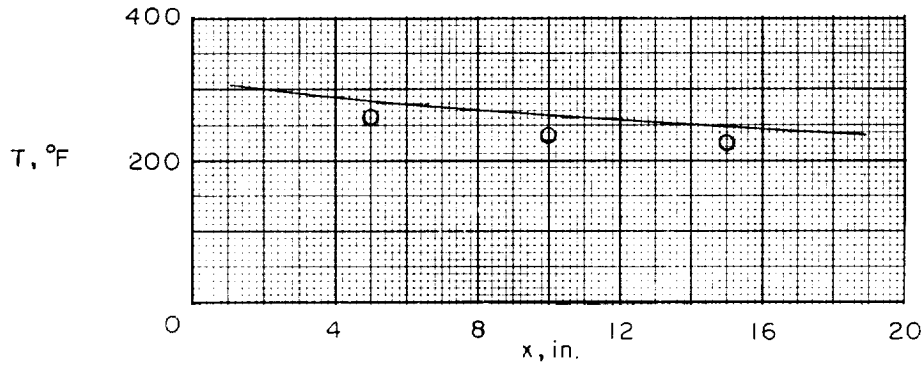

(c) t = 8 seconds; M = 1.98.

Figure 8.- Variation of skin temperature with distance from wing leading edge at various time intervals.

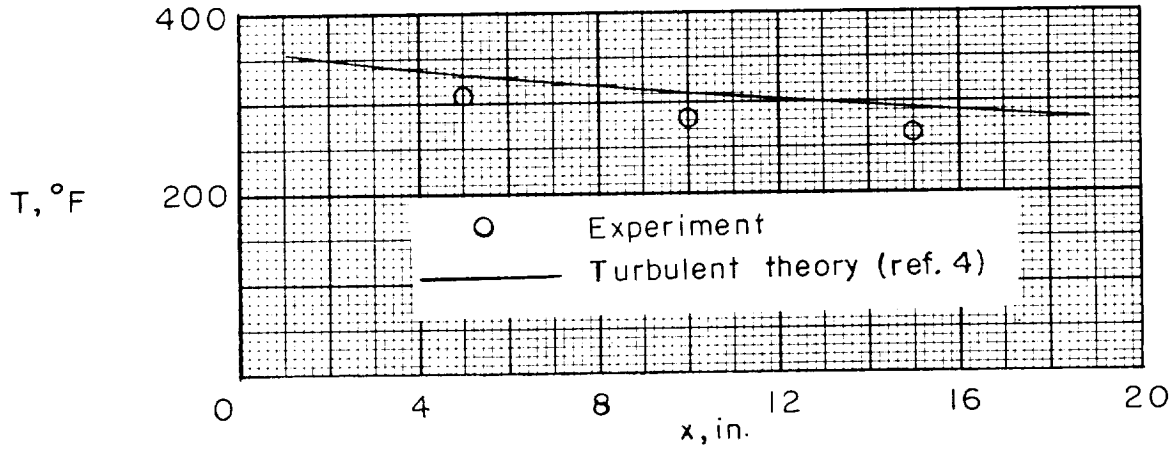

(d) t = 10 seconds; M = 2.18.

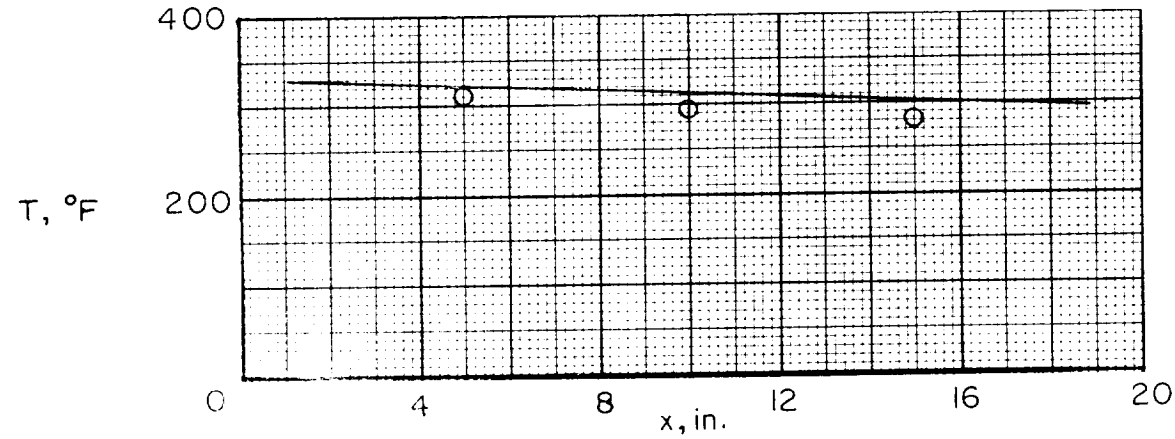

(e) t = 14 seconds; M = 1.35.

Figure 8.- Concluded.

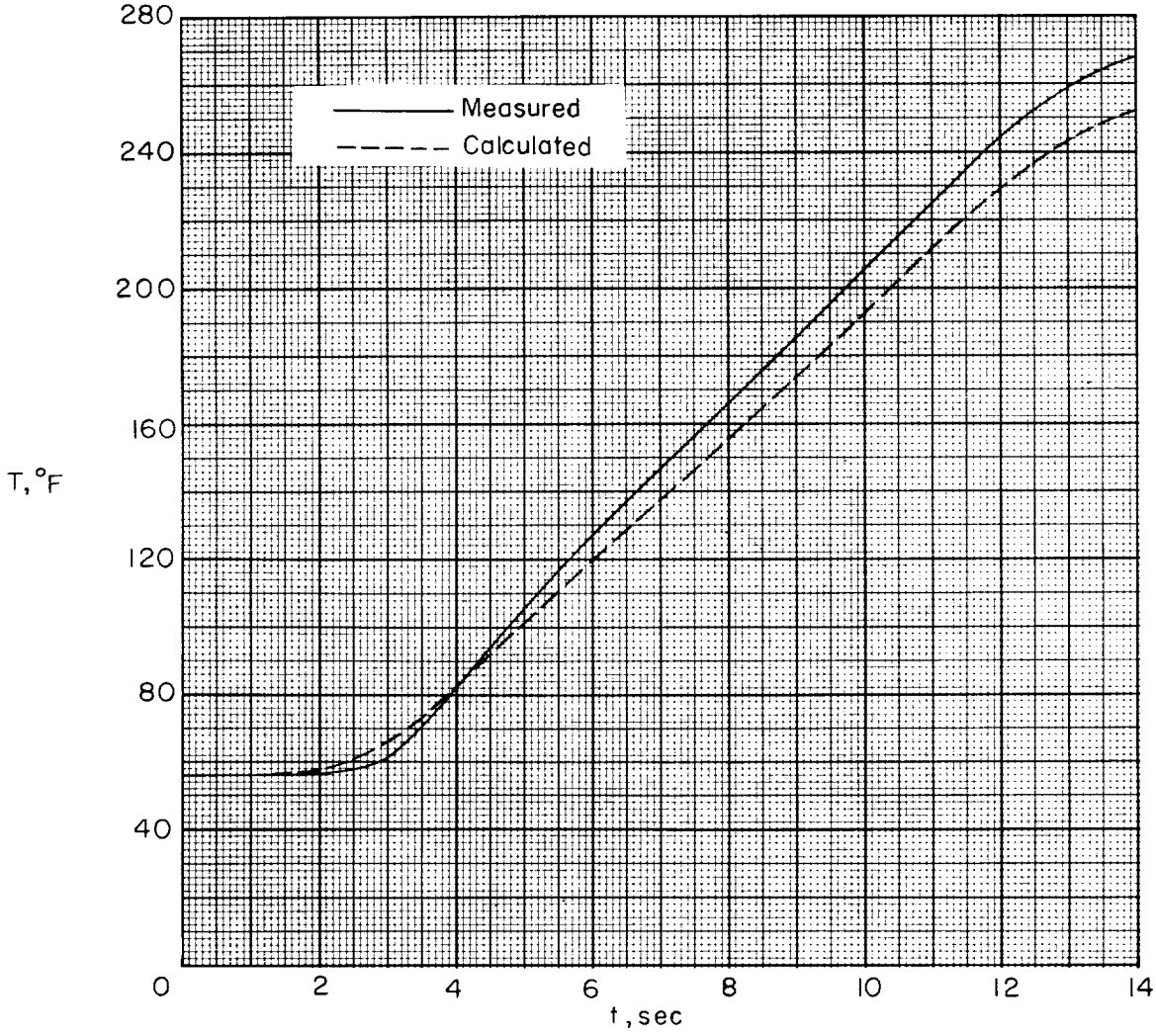

(a) Web center line.

Figure 9.- Comparison of measured temperatures with calculated temperatures.

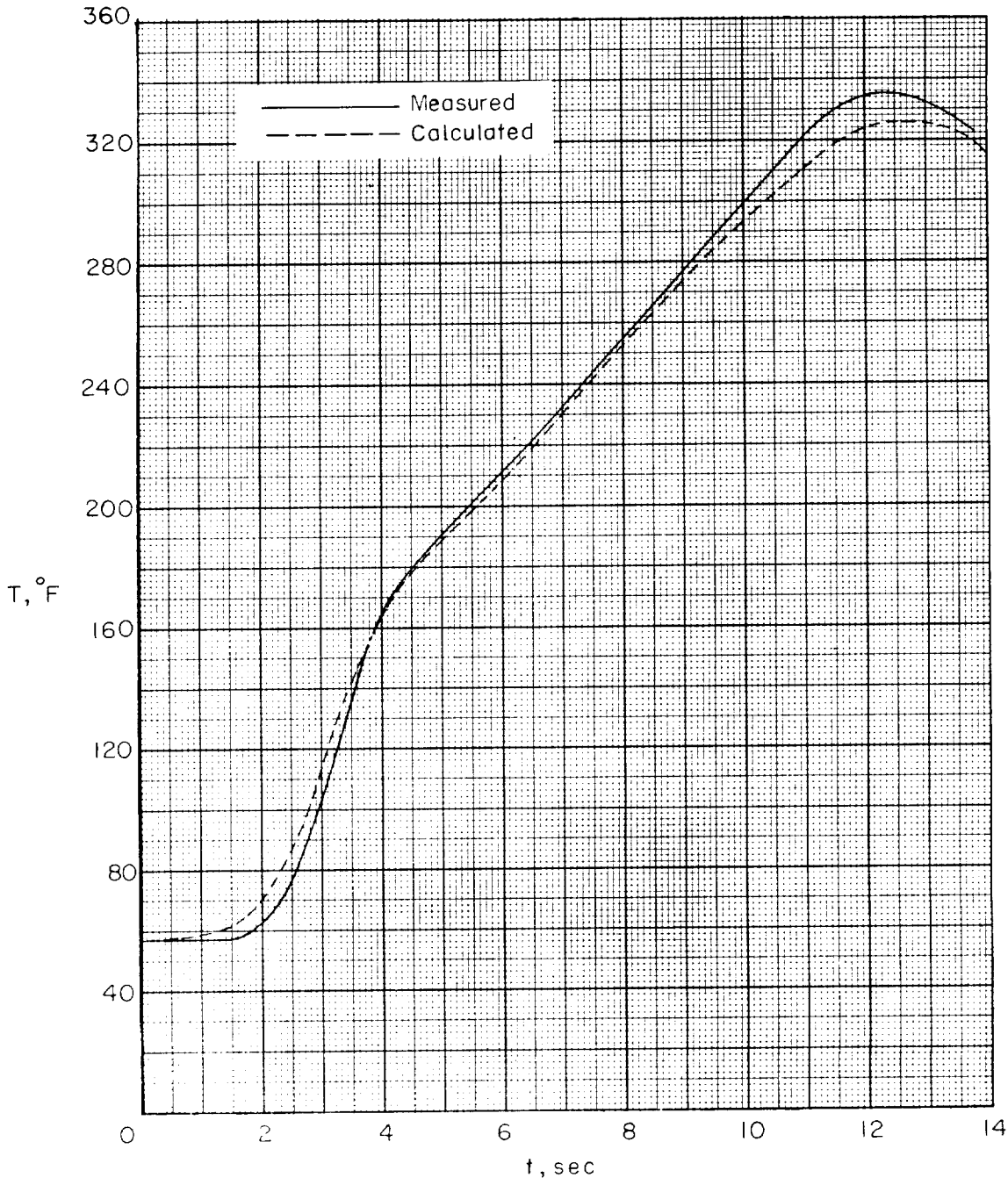

(b) Leading-edge wedge section.

Figure 9.- Continued.

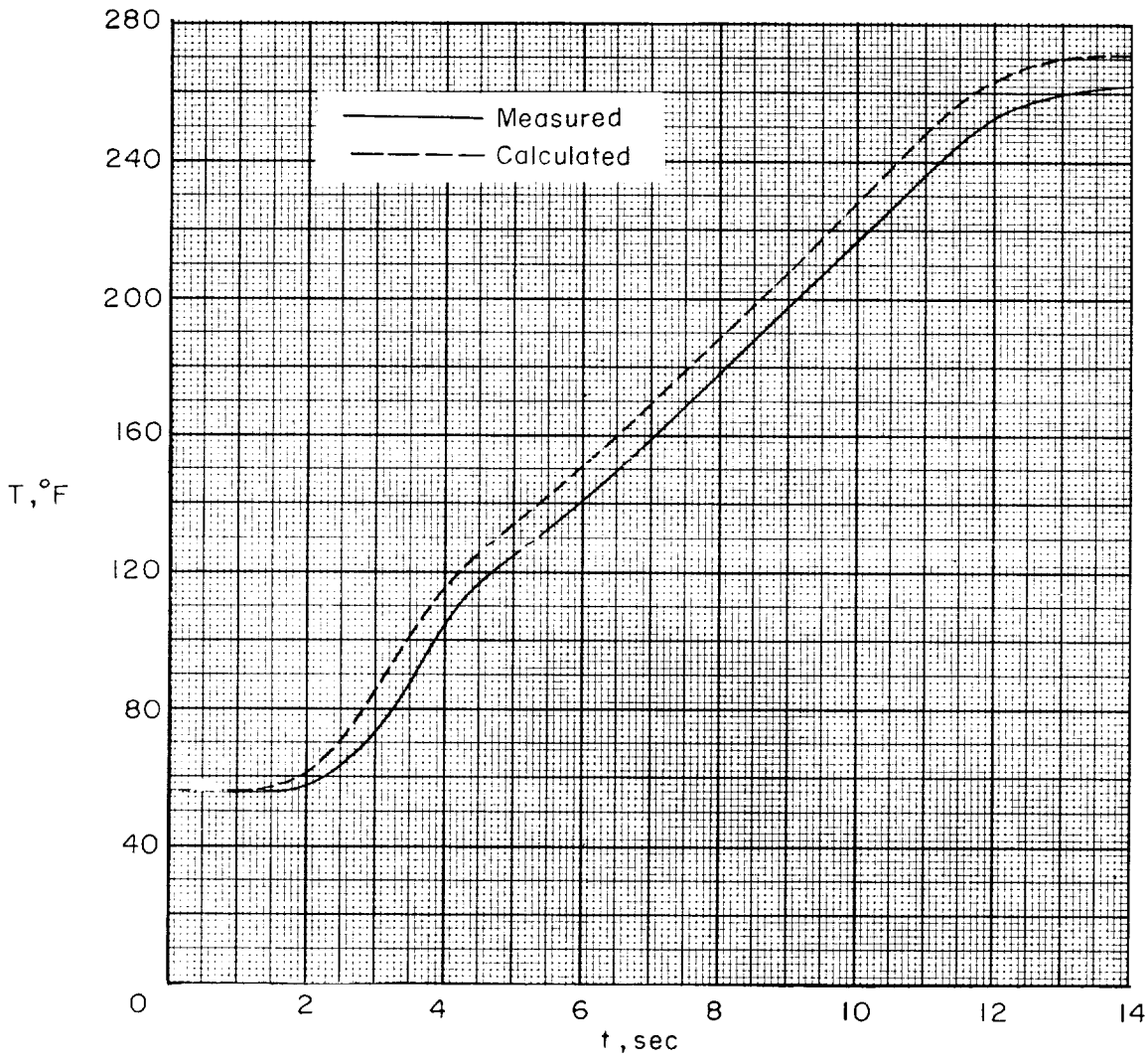

(c) Trailing-edge wedge section.

Figure 9.- Concluded.

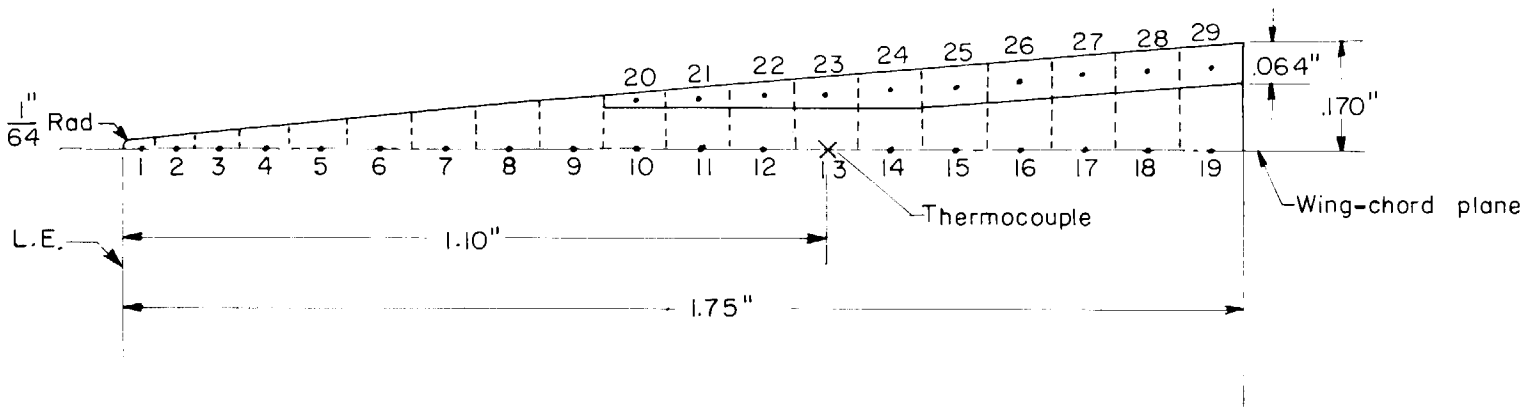

(a) Leading-edge wedge section.

Figure 10.- Sections of test wing in vicinity of internal thermocouples showing division elements for calculation purposes.

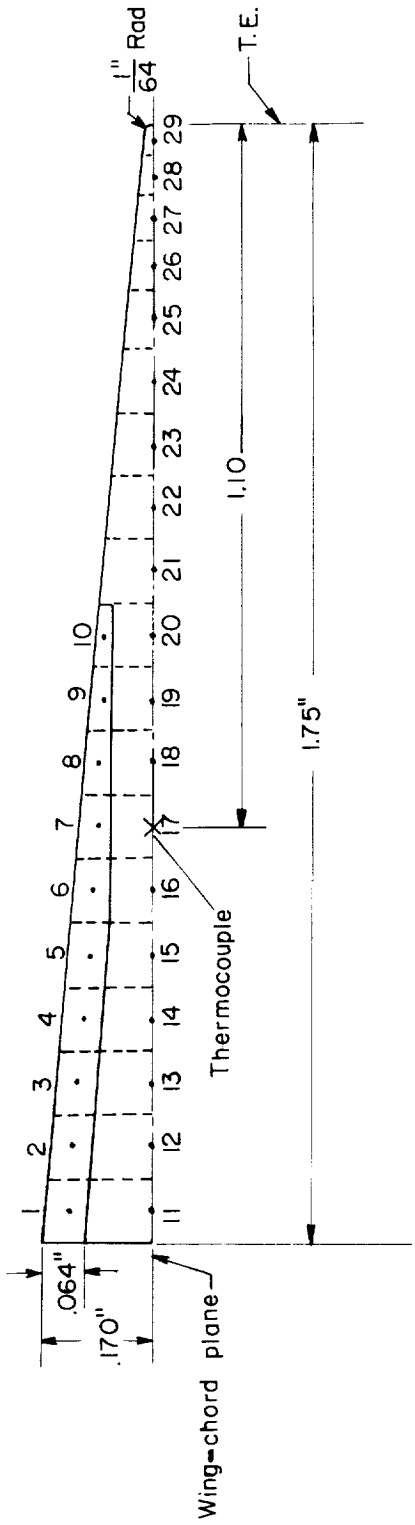

(b) Trailing-edge wedge section.

Figure 10.- Continued.

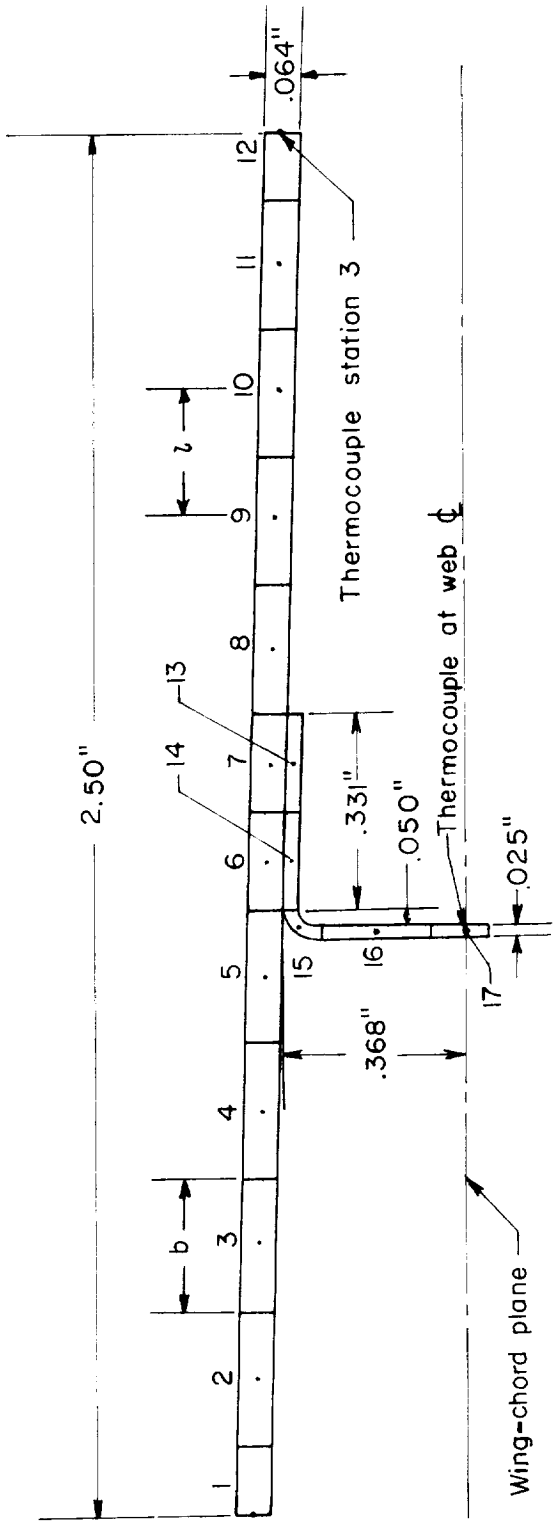

(c) Web section.

Figure 10.- Concluded.

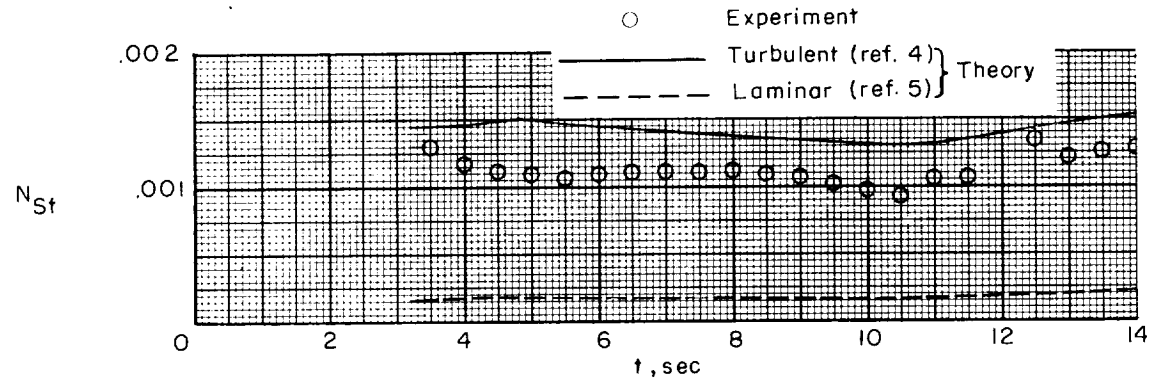

(a) Station 1.

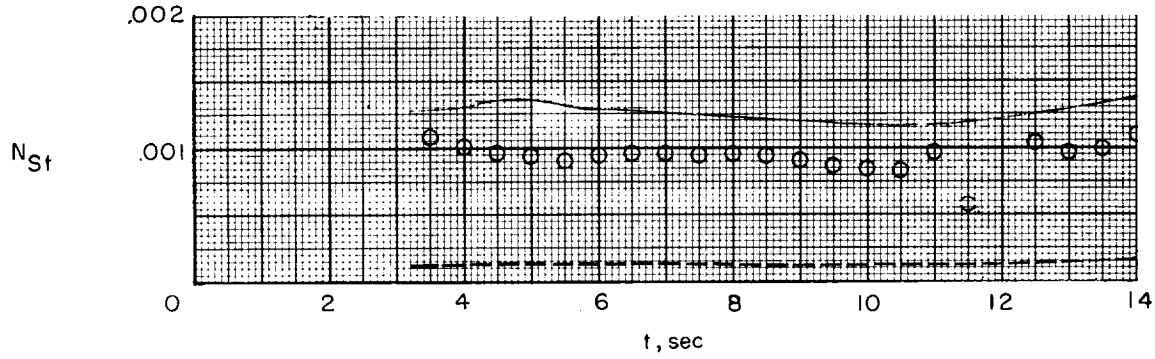

(b) Station 2.

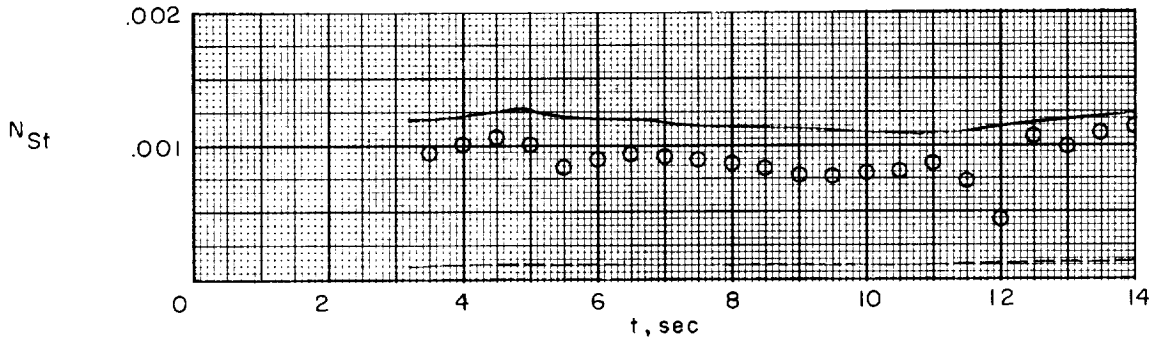

(c) Station 3.

Figure 11.- Variation of measured Stanton number with time and comparison with theoretical laminar and turbulent values.

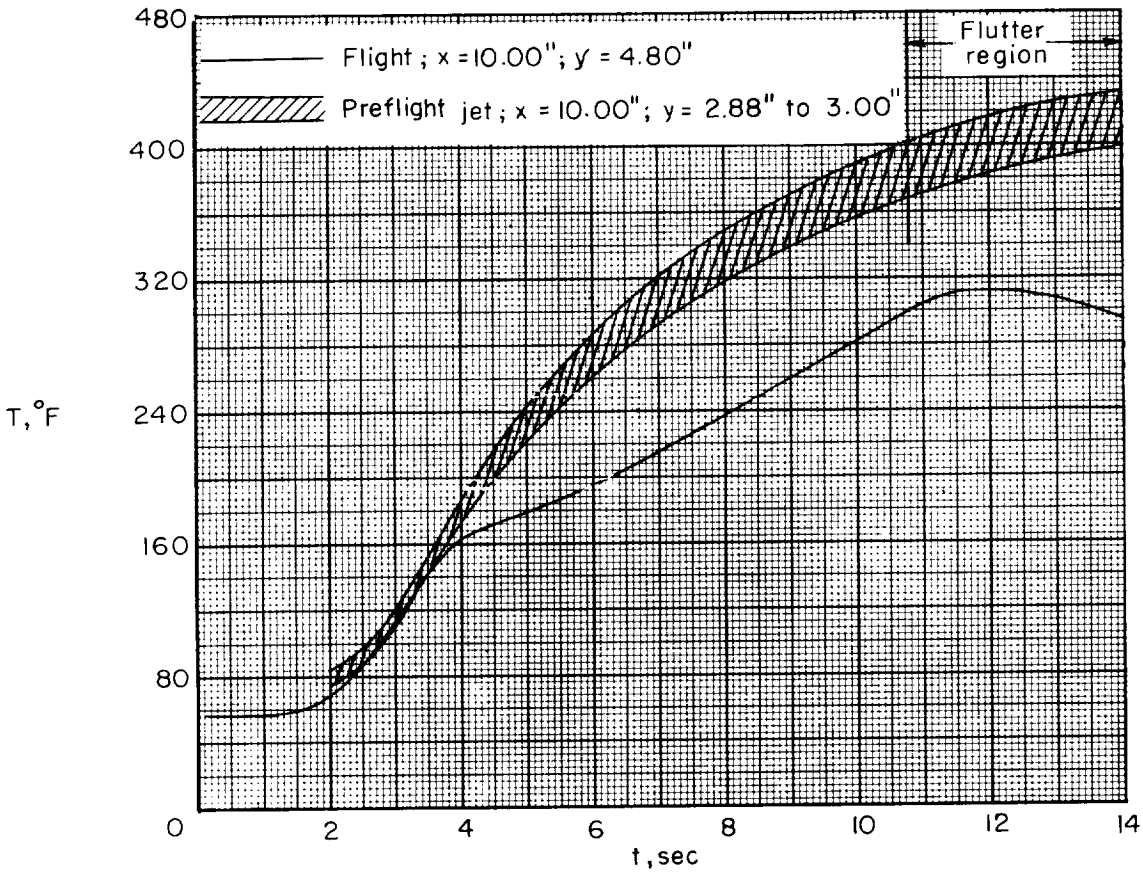

Figure 12.- Comparison of temperatures measured in flight and in preflight jet.

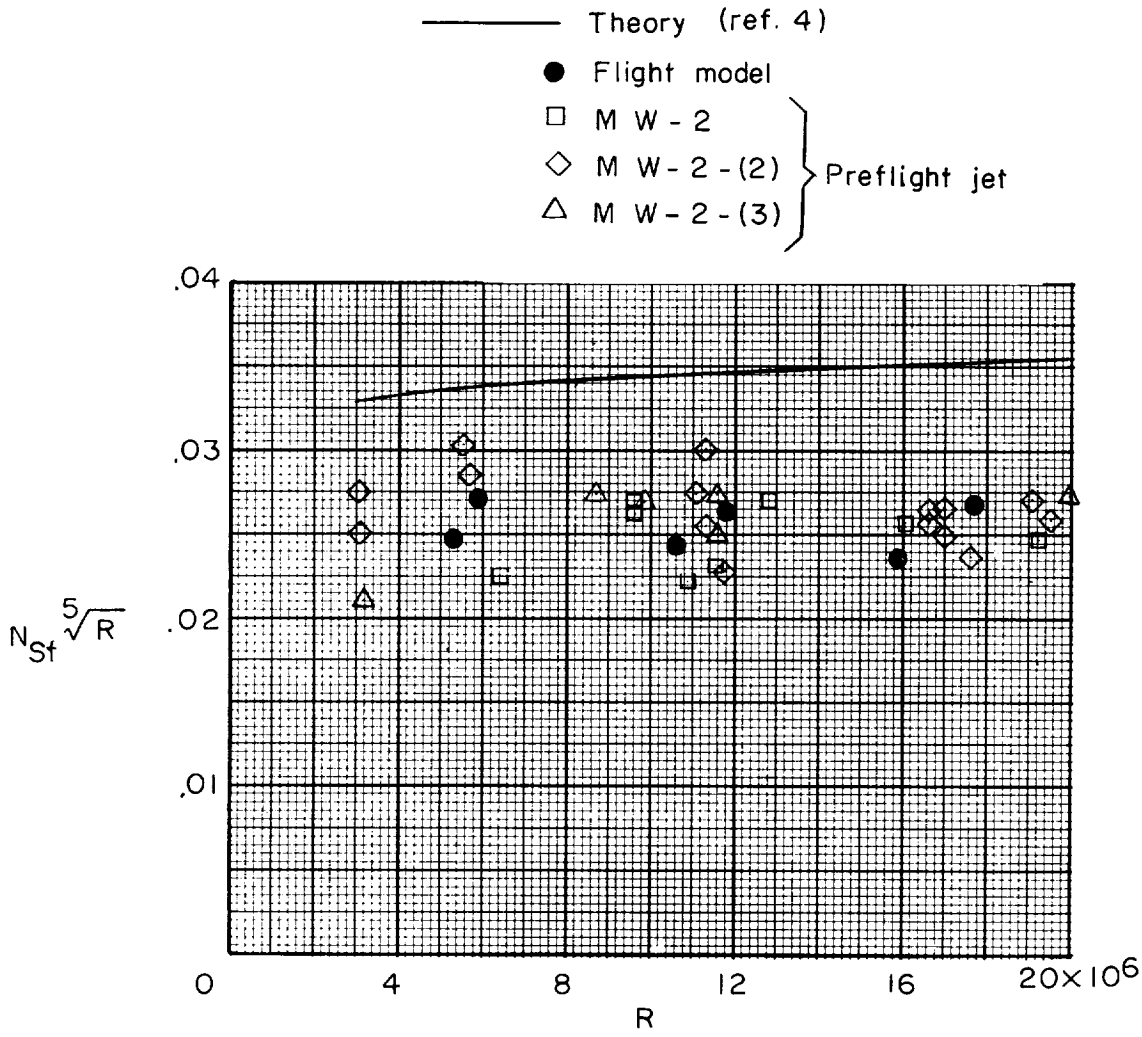

Figure 13.- Comparison of Stanton number values obtained in flight and in preflight jet. M = 2.0.

NASA MEMO 12-15-58L
National Aeronautics and Space Administration.
FREE-FLIGHT INVESTIGATION OF A ROCKET-PROPELLED MODEL TO DETERMINE THE AERODYNAMIC HEATING ON A THIN, UNSWEPT, UNTAPERED, MULTISPAR, ALUMINUM-ALLOY WING AT MACH NUMBERS UP TO 2.22. Emily W. Stephens. January 1959. 38p. diagrs., photos. (NASA MEMORANDUM 12-15-58L)

Aerodynamic heating data have been obtained for a thin, unswept, untapered, multispar, aluminum-alloy wing of a rocket-propelled model at Mach numbers up to 2.22. Temperature measurements made in the skin of the wing and in the internal structures agreed well with calculated values. Measured values of Stanton number were in reasonably good agreement with the theory of Van Driest for flat plates with turbulent boundary layers.

Copies obtainable from NASA, Washington

1. Heating, Aerodynamic (1.1.4.1)
2. Heat Transfer, Aerodynamic (1.1.4.2)
I. Stephens, Emily W.
II. NASA MEMO 12-15-58L

NASA

NASA MEMO 12-15-58L
National Aeronautics and Space Administration.
FREE-FLIGHT INVESTIGATION OF A ROCKET-PROPELLED MODEL TO DETERMINE THE AERODYNAMIC HEATING ON A THIN, UNSWEPT, UNTAPERED, MULTISPAR, ALUMINUM-ALLOY WING AT MACH NUMBERS UP TO 2.22. Emily W. Stephens. January 1959. 38p. diagrs., photos. (NASA MEMORANDUM 12-15-58L)

Aerodynamic heating data have been obtained for a thin, unswept, untapered, multispar, aluminum-alloy wing of a rocket-propelled model at Mach numbers up to 2.22. Temperature measurements made in the skin of the wing and in the internal structures agreed well with calculated values. Measured values of Stanton number were in reasonably good agreement with the theory of Van Driest for flat plates with turbulent boundary layers.

Copies obtainable from NASA, Washington

1. Heating, Aerodynamic (1.1.4.1)
2. Heat Transfer, Aerodynamic (1.1.4.2)
I. Stephens, Emily W.
II. NASA MEMO 12-15-58L

NASA

NASA MEMO 12-15-58L
National Aeronautics and Space Administration.
FREE-FLIGHT INVESTIGATION OF A ROCKET-PROPELLED MODEL TO DETERMINE THE AERODYNAMIC HEATING ON A THIN, UNSWEPT, UNTAPERED, MULTISPAR, ALUMINUM-ALLOY WING AT MACH NUMBERS UP TO 2.22. Emily W. Stephens. January 1959. 38p. diagrs., photos. (NASA MEMORANDUM 12-15-58L)

Aerodynamic heating data have been obtained for a thin, unswept, untapered, multispar, aluminum-alloy wing of a rocket-propelled model at Mach numbers up to 2.22. Temperature measurements made in the skin of the wing and in the internal structures agreed well with calculated values. Measured values of Stanton number were in reasonably good agreement with the theory of Van Driest for flat plates with turbulent boundary layers.

Copies obtainable from NASA, Washington

1. Heating, Aerodynamic (1.1.4.1)
2. Heat Transfer, Aerodynamic (1.1.4.2)
I. Stephens, Emily W.
II. NASA MEMO 12-15-58L

NASA

NASA MEMO 12-15-58L
National Aeronautics and Space Administration.
FREE-FLIGHT INVESTIGATION OF A ROCKET-PROPELLED MODEL TO DETERMINE THE AERODYNAMIC HEATING ON A THIN, UNSWEPT, UNTAPERED, MULTISPAR, ALUMINUM-ALLOY WING AT MACH NUMBERS UP TO 2.22. Emily W. Stephens. January 1959. 38p. diagrs., photos. (NASA MEMORANDUM 12-15-58L)

Aerodynamic heating data have been obtained for a thin, unswept, untapered, multispar, aluminum-alloy wing of a rocket-propelled model at Mach numbers up to 2.22. Temperature measurements made in the skin of the wing and in the internal structures agreed well with calculated values. Measured values of Stanton number were in reasonably good agreement with the theory of Van Driest for flat plates with turbulent boundary layers.

Copies obtainable from NASA, Washington

1. Heating, Aerodynamic (1.1.4.1)
2. Heat Transfer, Aerodynamic (1.1.4.2)
I. Stephens, Emily W.
II. NASA MEMO 12-15-58L

NASA